Comanche Peak Units 1 and 2 Heatup and Cooldown Limit Curves for Normal Operation

Westinghouse

WCAP-16346-NP, Revision 0

Comanche Peak Units 1 and 2
Heatup and Cooldown Limit Curves
for Normal Operation

T. J. Laubham
E.T. Hayes

NOVEMBER 2004
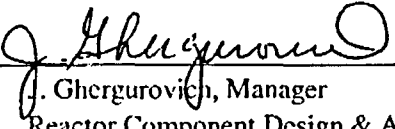
Approved: _J. Ghergurovich, Manager_
Reactor Component Design & Analysis

PREFACE

This report has been technically reviewed and verified by:

C.M. Burton _Cupt_

RECORD OF REVISION

Revision 0:   Original Issue

TABLE OF CONTENTS

LIST OF TABLES

LIST OF TABLES – (continued)

LIST OF FIGURES

EXECUTIVE SUMMARY

This report provides the methodology and results of the generation of heatup and cooldown pressure temperature (PT) limit curves for normal operation of the Comanche Peak Units 1 and 2 reactor vessels. The PT curves were generated based on the latest available reactor vessel information and updated calculated fluences. The new Comanche Peak Units 1 and 2 heatup and cooldown pressure-temperature limit curves were generated using the "axial flaw" methodology of 1998 ASME Code, Section XI through the 2000 Addenda, which allows the use of the K_{Ic} methodology. The material with the highest adjusted reference temperature (ART) was the Unit 1 Intermediate Shell Plate R-1107-1. The PT limit curves were generated for 36 EFPY using heatup rates of 20, 60 and 100°F/hr and cooldown rates of 0, 20, 40, 60 and 100°F/hr. Lastly, two sets of PT Curves are provided, one with the flange notch requirement and one without. These curves can be found in Figures 6-1 through 6-4.

1   INTRODUCTION

Heatup and cooldown limit curves are calculated using the adjusted RT_{NDT} (reference nil-ductility temperature) corresponding to the limiting beltline region material of the reactor vessel. The adjusted RT_{NDT} of the limiting material in the core region of the reactor vessel is determined by using the unirradiated reactor vessel material fracture toughness properties, estimating the radiation-induced ΔRT_{NDT}, and adding a margin. The unirradiated RT_{NDT} is designated as the higher of either the drop weight nil-ductility transition temperature (NDTT) or the temperature at which the material exhibits at least 50 ft-lb of impact energy and 35-mil lateral expansion (normal to the major working direction) minus 60°F.

RT_{NDT} increases as the material is exposed to fast-neutron radiation. Therefore, to find the most limiting RT_{NDT} at any time period in the reactor's life, ΔRT_{NDT} due to the radiation exposure associated with that time period must be added to the unirradiated RT_{NDT} (IRT_{NDT}). The extent of the shift in RT_{NDT} is enhanced by certain chemical elements (such as copper and nickel) present in reactor vessel steels. The Nuclear Regulatory Commission (NRC) has published a method for predicting radiation embrittlement in Regulatory Guide 1.99, Revision 2, "Radiation Embrittlement of Reactor Vessel Materials."[1] Regulatory Guide 1.99, Revision 2, is used for the calculation of Adjusted Reference Temperature (ART) values (IRT_{NDT} + ΔRT_{NDT} + margins for uncertainties) at the 1/4T and 3/4T locations, where T is the thickness of the vessel at the beltline region measured from the clad/base metal interface.

The heatup and cooldown curves documented in this report were generated using the most limiting ART values and the NRC approved methodology documented in WCAP-14040-NP-A, Revision 4[2], "Methodology Used to Develop Cold Overpressure Mitigating System Setpoints and RCS Heatup and Cooldown Limit Curves."

The purpose of this report is to present the calculations and the development of the Comanche Peak Units 1 and 2 heatup and cooldown curves for 36 EFPY. This report documents the calculated ART values and the development of the PT limit curves for normal operation. The PT curves herein were generated without instrumentation errors. The PT curves include a hydrostatic leak test limit curve from 2485 psig to 2000 psig, along with the pressure-temperature limits for the vessel flange region per the requirements of 10 CFR Part 50, Appendix G[3].

2   FRACTURE TOUGHNESS PROPERTIES

The fracture-toughness properties of the ferritic materials in the reactor coolant pressure boundary are determined in accordance with the NRC Standard Review Plan[4]. The beltline material properties of the Comanche Peak Units 1 and 2 reactor vessel are presented in Table 2-1.

Best estimate copper (Cu) and nickel (Ni) weight percent values used to calculate chemistry factors (CF) in accordance with Regulatory Guide 1.99, Revision 2, are provided in Table 2-1. Additionally, surveillance capsule data is available for two capsules already removed from both Comanche Peak reactor vessels. This surveillance capsule data was also used to calculate CF values per Position 2.1 of Regulatory Guide 1.99, Revision 2 in Tables 2-3 and 2-4. These CF values are summarized in Table 2-5.

The Regulatory Guide 1.99, Revision 2 methodology used to develop the heatup and cooldown curves documented in this report is the same as that documented in WCAP-14040, Revision 4. The chemistry factors (CFs) were calculated using Regulatory Guide 1.99 Revision 2, Positions 1.1 and 2.1. Position 1.1 uses the Tables from the Reg. Guide along with the best estimate copper and nickel weight percents, which are presented in Table 2-1. Position 2.1 uses the surveillance capsule data from all capsules withdrawn to date. The fluence values used to determine the CFs in Tables 2-3 and 2-4 are the calculated fluence values at the surveillance capsule locations. Hence, the calculated fluence values were used for all cases. Included in Table 2-2 are the Calculated Capsule fluence values for Comanche Peak Units 1 and 2. All capsule fluence values were determined using ENDF/B-VI cross-sections and followed the guidance in Regulatory Guide 1.190[9].

It should be noted that in the calculations of chemistry factors in Tables 2-3 and 2-4, the ratio was applied to account for chemistry differences between the vessel weld material and the surveillance weld material. As far as temperature adjustments are concerned, the Comanche Peak Units 1 and 2 data does not require any adjustments since it is being applied to their own plants.

TABLE 2-1
Summary of the Best Estimate Cu and Ni Weight Percent and Initial RT_{NDT} Values for the
Comanche Peak Units 1 and 2 Reactor Vessel Materials

Material Description	Cu (%)[a]	Ni(%)[a]	Initial RT_{NDT}[a]
Comanche Peak Unit 1			
Closure Head Flange R-1102-1	---	0.77	40°F
Vessel Flange R-1101-1	---	0.72	10°F
Intermediate Shell Plate R-1107-1[b]	0.07	0.62	10°F
Intermediate Shell Plate R-1107-2[b]	0.07	0.67	-10°F
Intermediate Shell Plate R-1107-3[b]	0.06	0.65	10°F
Lower Shell Plate R-1108-1[b]	0.08	0.65	0°F
Lower Shell Plate R-1108-2[b]	0,06	0.60	20°F
Lower Shell Plate R-1108-3[b]	0.08	0.65	0°F
Beltline Region Weld Metal[c]	0.045	0.20	-70°F
Surveillance Program Weld Metal[c]	0.04	0.22	---
Comanche Peak Unit 2			
Closure Head Flange R-3802-1	---	0.71	40°F
Vessel Flange R-3801-1	---	0.70	-10°F
Intermediate Shell Plate R3807-1	0.06	0.64	-20°F
Intermediate Shell Plate R3807-2	0.06	0.64	10°F
Intermediate Shell Plate R3807-3	0.05	0.60	-20°F
Lower Shell Plate R3816-1	0.05	0.59	-30°F
Lower Shell Plate R3816-2	0.03	0.65	0°F
Lower Shell Plate R3816-3	0.04	0.63	-40°F
Intermediate & Lower Shell Longitudinal Welds[d]	0.046	0.059	-50°F
Intermediate to Lower Shell Girth Weld[d]	0.046	0.059	-60°F
Comanche Peak Unit 2 Surveillance Weld Metal[d]	0.035	0.091	---

Notes: See Next Page

Notes for Table 2-1:

(a) Based on Measured Data.

(b) The Cu & Ni weight percent for all intermediate and lower shell plates were calculated from the average of two data points listed on the Combustion Engineering (CE) Certified Material Test Report (CMTR), which are listed in Reference 5. Note that these are different values than those provided to the NRC from TXU in their 92-01 response (See Reference 6). However, the values listed above will produce an equal or more conservative Chemistry Factor (CF).

(c) All Unit 1 weld metal was fabricated with weld wire type B4, heat # 88112, flux type Linde 0091, and flux lot number 0145. The best estimate Cu & Ni for the beltline region welds was taken from Reference 7, which was originally documented in CE Report NPSD-1039[8].

(d) The Unit 2 surveillance weld was made with the same weld wire and flux as the intermediate to lower shell girth weld (*weld wire heat # 89833, flux type Linde 124*). The longitudinal welds seams were also made with weld heat # 89833, but with flux type Linde 0091. The best estimate Cu & Ni for the beltline region welds was taken from Reference 7, which was originally documented in CE Report NPSD-1039[8]

TABLE 2-2

Calculated Integrated Neutron Exposure of the Surveillance Capsules @ Comanche Peak Units 1 and 2

Capsule	Fluence
Comanche Peak Unit 1[a]	
U	3.18×10^{18} n/cm^2, (E > 1.0 MeV)
Y	1.49×10^{19} n/cm^2, (E > 1.0 MeV)
Comanche Peak Unit 2[b]	
U	3.15×10^{18} n/cm^2, (E > 1.0 MeV)
X	2.20×10^{19} n/cm^2, (E > 1.0 MeV)

NOTES:

(a)   See Section 3, Table 3-5.

(b)   Per WCAP-16277-NP[10].

TABLE 2-3

Calculation of CF Values using Comanche Peak Unit 1 Surveillance Capsule Test Results

Material	Capsule	F[a]	FF[a]	ΔRT_{NDT}[c]	FF x ΔRT_{NDT}	FF[2]
Lower Shell R1108-2	U	0.318	0.683	6.6	4.521	0.469
(*Longitudinal*)	Y	1.49	1.11	6.9	7.66	1.23
Lower Shell R1108-2	U	0.318	0.683	21.3	14.591	0.469
(*Transverse*)	Y	1.49	1.11	25.3	28.08	1.23
				SUM	54.852	3.398
$CF_{R1108-2} = \sum(FF \times \Delta RT_{NDT}) \div \sum(FF^2) = 54.852 \div 3.398 = 16.1°F$						
Weld Metal	U	0.318	0.683	0.0[d,e]	0.0	0.469
(*Heat # 88112*)	Y	1.49	1.11	17.6[d]	19.54	1.23
				SUM	19.54	1.699
$CF_{WELD} = \sum(FF \times \Delta RT_{NDT}) \div \sum(FF^2) = 19.54 \div 1.699 = 11.5°F$						

Notes:

(a)   F = Calculated Fluence (10^{19} n/cm^2, E > 1.0 MeV). See Table 2-2

(b)   FF = Fluence Factor = $F^{(0.28 - 0.1 * \log F)}$

(c)   All available data is from Comanche Peak Unit 1[11]. Therefore, no temperature adjustment is required.

(d)   The measured ΔRT_{NDT} values for the weld metal have been adjusted by a ratio of 1.04.

(e)   The CVGRAPH calculated value is -14.14°F. 0.0°F was used in the calculation for conservatism.

[*Note that the CF from the previous analysis in Reference 11 was 15.7°F for the surveillance lower shell plate and 10.7°F for the surveillance weld. As can be seen above there is only a minor change (i.e., <1°F) to the CF values. Thus, the credibility evaluation from the previous analysis remains valid...All Unit 1 surveillance data is credible.*]

TABLE 2-4

Calculation of CF values using Comanche Peak Unit 2 Surveillance Capsule Data

Material	Capsule	$F^{(a)}$	$FF^{(a)}$	$\Delta RT_{NDT}^{(c)}$	$FF \times \Delta RT_{NDT}$	FF^2
Inter. Shell R3807-2	U	0.315	0.683	1.6	1.093	0.466
(*Longitudinal*)	X	2.20	1.21	1.6	1.94	1.46
Inter. Shell R3807-2	U	0.315	0.683	23.4	15.982	0.466
(*Transverse*)	X	2.20	1.21	52.9	64.01	1.46
				SUM	83.025	3.852
$CF_{R3807-2} = \Sigma(FF \times \Delta RT_{NDT}) \div \Sigma(FF^2) = 83.025 \div 3.852 = 21.6°F$						
Weld Metal	U	0.315	0.683	3.74[(d)]	2.55	0.466
(*Heat # 89833*)	X	2.20	1.21	50.13[(d)]	60.66	1.46
				SUM	63.21	1.926
$CF_{WELD} = \Sigma(FF \times \Delta RT_{NDT}) \div \Sigma(FF^2) = 63.21 \div 1.926 = 32.8°F$						

Notes:

(a) F = Calculated Fluence. Units are x 10^{19} n/cm^2 (E > 1.0 MeV). See Table 2-2.

(b) FF = Fluence Factor = $f^{(0.28 - 0.1*\log f)}$.

(c) All available data is from Comanche Peak Unit 2[10]. Therefore, no temperature adjustment is required.

(d) The measured ΔRT_{NDT} values for the weld metal have been adjusted by a ratio of 1.04.

TABLE 2-5
Summary of the Comanche Peak Units 1 and 2 Reactor Vessel Beltline Material Chemistry Factors

Material	Reg. Guide 1.99, Rev. 2 Position 1.1 CF's	Reg. Guide 1.99, Rev. 2 Position 2.1 CF's
Comanche Peak Unit 1		
Intermediate Shell Plate R-1107-1 (*Heat # C4021-1*)	44°F	- - -
Intermediate Shell Plate R-1107-2 (*Heat # B7854-1*)	44°F	- - -
Intermediate Shell Plate R-1107-3 (*Heat # C4106-2*)	37°F	- - -
Lower Shell Plate R-1108-1 (*Heat # C4464-1*)	51°F	- - -
Lower Shell Plate R-1108-2 (*Heat # C4533-2*)	37°F	16.1°F
Lower Shell Plate R-1108-3 (*Heat # C4589-1*)	51°F	- - -
All Beltline Region Welds (*Heat # 88112*)	46°F	11.5°F
Comanche Peak Unit 2		
Intermediate Shell Plate R3807-1 (*Heat # C5522-1*)	37°F	- - -
Intermediate Shell Plate R3807-2 (*Heat # C5522-2*)	37°F	21.6°F
Intermediate Shell Plate R3807-3 (*Heat # B9566-1*)	31°F	- - -
Lower Shell Plate R3816-1 (*Heat # NR64435-1*)	31°F	- - -
Lower Shell Plate R3816-2 (*Heat # NR64439-1*)	20°F	- - -
Lower Shell Plate R3816-3 (*Heat # NR64443-1*)	26°F	- - -
Intermediate & Lower Shell Longitudinal Welds (*Heat # 89833*)	31.5°F	32.8°F
Intermediate to Lower Shell Girth Weld (*Heat # 89833*)	31.5°F	32.8°F

3   RADIATION ANALYSIS AND NEUTRON DOSIMETRY (UNIT 1)

3.1   INTRODUCTION

This section describes a discrete ordinates S_n transport analysis performed for the Comanche Peak Unit 1 reactor to determine the neutron radiation environment within the reactor pressure vessel and surveillance capsules. In this analysis, fast neutron exposure parameters in terms of fast neutron fluence (E > 1.0 MeV) and iron atom displacements (dpa) were established on a plant and fuel cycle specific basis. In addition, neutron dosimetry sensor sets from the first two surveillance capsules withdrawn from the Comanche Peak Unit 1 reactor were re-analyzed using the current dosimetry evaluation methodology. These dosimetry updates are presented in Appendix A of this report. Comparisons of the results from these dosimetry evaluations with the analytical predictions served to validate the plant specific neutron transport calculations. These validated calculations subsequently formed the basis for providing projections of the neutron exposure of the reactor pressure vessel for operating periods extending to 54 Effective Full Power Years (EFPY).

The use of fast neutron fluence (E > 1.0 MeV) to correlate measured material property changes to the neutron exposure of the material has traditionally been accepted for the development of damage trend curves as well as for the implementation of trend curve data to assess the condition of the vessel. In recent years, however, it has been suggested that an exposure model that accounts for differences in neutron energy spectra between surveillance capsule locations and positions within the vessel wall could lead to an improvement in the uncertainties associated with damage trend curves and improved accuracy in the evaluation of damage gradients through the reactor vessel wall.

Because of this potential shift away from a threshold fluence toward an energy dependent damage function for data correlation, ASTM Standard Practice E853, "Analysis and Interpretation of Light-Water Reactor Surveillance Results," recommends reporting displacements per iron atom (dpa) along with fluence (E > 1.0 MeV) to provide a database for future reference. The energy dependent dpa function to be used for this evaluation is specified in ASTM Standard Practice E693, "Characterizing Neutron Exposures in Iron and Low Alloy Steels in Terms of Displacements per Atom." The application of the dpa parameter to the assessment of embrittlement gradients through the thickness of the reactor vessel wall has already been promulgated in Revision 2 to Regulatory Guide 1.99, "Radiation Embrittlement of Reactor Vessel Materials."

All of the calculations and dosimetry evaluations described in this section and in Appendix A were based on the latest available nuclear cross-section data derived from ENDF/B-VI and made use of the latest available calculational tools. Furthermore, the neutron transport and dosimetry evaluation methodologies follow the guidance of Regulatory Guide 1.190, "Calculational and Dosimetry Methods for Determining Pressure Vessel Neutron Fluence."[9] Additionally, the methods used to develop the calculated pressure vessel fluence are consistent with the NRC approved methodology described in WCAP-14040-NP-A, "Methodology Used to Develop Cold Overpressure Mitigating System Setpoints and RCS Heatup and Cooldown Limit Curves," May 2004.[2]

3.2 DISCRETE ORDINATES ANALYSIS

Six irradiation capsules attached to the neutron pad are included in the reactor design that constitutes the reactor vessel surveillance program. The capsules are located at azimuthal angles of 58.5°, 61°, 121.5°, 238.5°, 241°, and 301.5°. These full core positions correspond to the following octant symmetric locations represented in Figure 3-1: 29° from the core cardinal axes (for the 61° and 241° dual surveillance capsule holder locations found in octants with a 22.5° neutron pad segment) and 31.5° from the core cardinal axes (for the 121.5° and 301.5° single surveillance capsule holder locations found in octants with a 20.0° neutron pad segment, and for the 58.5° and the 238.5° dual surveillance capsule holder locations found in octants with a 22.5° neutron pad segment). The stainless steel specimen containers are 1.182-inch by 1-inch and are approximately 56 inches in height. The containers are positioned axially such that the test specimens are centered on the core midplane, thus spanning the central 5 feet of the 12-foot high reactor core.

From a neutronic standpoint, the surveillance capsules and associated support structures are significant. The presence of these materials has a marked effect on both the spatial distribution of neutron flux and the neutron energy spectrum in the water annulus between the neutron pads and the reactor vessel. In order to determine the neutron environment at the test specimen location, the capsules themselves must be included in the analytical model.

In performing the fast neutron exposure evaluations for the Comanche Peak Unit 1 reactor vessel and surveillance capsules, a series of fuel cycle specific forward transport calculations were carried out using the following three-dimensional flux synthesis technique:

$$\varphi(r,\theta,z) = \varphi(r,\theta) * \frac{\varphi(r,z)}{\varphi(r)}$$

where $\varphi(r,\theta,z)$ is the synthesized three-dimensional neutron flux distribution, $\varphi(r,\theta)$ is the transport solution in r,θ geometry, $\varphi(r,z)$ is the two-dimensional solution for a cylindrical reactor model using the actual axial core power distribution, and $\varphi(r)$ is the one-dimensional solution for a cylindrical reactor model using the same source per unit height as that used in the r,θ two-dimensional calculation. This synthesis procedure was carried out for each operating cycle at Comanche Peak Unit 1.

For the Comanche Peak Unit 1 transport calculations, the r,θ models depicted in Figure 3-1 were utilized since, with the exception of the neutron pads, the reactor is octant symmetric. These r,θ models include the core, the reactor internals, the neutron pads – including explicit representations of octants not containing surveillance capsules and octants with surveillance capsules at 29° and 31.5°, the pressure vessel cladding and vessel wall, the insulation external to the pressure vessel, and the primary biological shield wall. These models formed the basis for the calculated results and enabled making comparisons to the surveillance capsule dosimetry evaluations. In developing these analytical models, nominal design dimensions were employed for the various structural components. Likewise, water temperatures, and hence, coolant densities in the reactor core and downcomer regions of the reactor were taken to be representative of full power operating conditions. The coolant densities were treated on a fuel cycle specific basis. The reactor core itself was treated as a homogeneous mixture of fuel, cladding, water, and miscellaneous core structures such as fuel assembly grids, guide tubes, et cetera. The geometric mesh description of the r,θ reactor models consisted of 183 radial by 99 azimuthal intervals. Mesh sizes were chosen to assure that

proper convergence of the inner iterations was achieved on a point-wise basis. The point-wise inner iteration flux convergence criterion utilized in the r,θ calculations was set at a value of 0.001.

The r,z model used for the Comanche Peak Unit 1 calculations is shown in Figure 3-2 and extends radially from the centerline of the reactor core out to a location interior to the primary biological shield and over an axial span from an elevation below the lower core plate to above the upper core plate. As in the case of the r,θ models, nominal design dimensions and full power coolant densities were employed in the calculations. In this case, the homogenous core region was treated as an equivalent cylinder with a volume equal to that of the active core zone. The stainless steel former plates located between the core baffle and core barrel regions were also explicitly included in the model. The r,z geometric mesh description of these reactor models consisted of 153 radial by 188 axial intervals. As in the case of the r,θ calculations, mesh sizes were chosen to assure that proper convergence of the inner iterations was achieved on a point-wise basis. The point-wise inner iteration flux convergence criterion utilized in the r,z calculations was also set at a value of 0.001.

The one-dimensional radial model used in the synthesis procedure consisted of the same 153 radial mesh intervals included in the r,z model. Thus, radial synthesis factors could be determined on a mesh-wise basis throughout the entire geometry.

The core power distributions used in the plant specific transport analysis were provided by TXU Electric for each of the first ten fuel cycles at Comanche Peak Unit 1[14-18]. Specifically, the data utilized included cycle dependent fuel assembly initial enrichments, burn-ups, and axial power distributions. This information was used to develop spatial and energy dependent core source distributions averaged over each individual fuel cycle. Therefore, the results from the neutron transport calculations provided data in terms of fuel cycle averaged neutron flux, which when multiplied by the appropriate fuel cycle length, generated the incremental fast neutron exposure for each fuel cycle. In constructing these core source distributions, the energy distribution of the source was based on an appropriate fission split for uranium and plutonium isotopes based on the initial enrichment and burn-up history of individual fuel assemblies. From these assembly dependent fission splits, composite values of energy release per fission, neutron yield per fission, and fission spectrum were determined.

All of the transport calculations supporting this analysis were carried out using the DORT discrete ordinates code Version 3.1[19] and the BUGLE-96 cross-section library.[20] The BUGLE-96 library provides a 67 group coupled neutron-gamma ray cross-section data set produced specifically for light water reactor (LWR) applications. In these analyses, anisotropic scattering was treated with a P_5 legendre expansion and angular discretization was modeled with an S_{16} order of angular quadrature. Energy and space dependent core power distributions, as well as system operating temperatures, were treated on a fuel cycle specific basis.

Selected results from the neutron transport analyses are provided in Tables 3-1 through 3-6. In Table 3-1, the calculated exposure rates and integrated exposures, expressed in terms of both neutron fluence (E > 1.0 MeV) and dpa, are given at the radial and azimuthal center of the octant symmetric surveillance capsule positions, i.e., for the 29° dual capsule, 31.5° dual capsule, and 31.5° single capsule. These results, representative of the axial midplane of the active core, establish the calculated exposure of the surveillance capsules withdrawn to date as well as projected into the future. Similar information is provided in Table 3-2 for the reactor vessel inner radius at five azimuthal locations. The vessel data given

in Table 3-2 were taken at the clad/base metal interface, and thus, represent maximum calculated exposure levels on the vessel.

From the data provided in Table 3-2 it is noted that the peak clad/base metal interface vessel fluence (E > 1.0 MeV) at the end of the tenth fuel cycle (i.e., after 11.69 EFPY of plant operation) was 7.26×10^{18} n/cm^2.

Both calculated fluence (E > 1.0 MeV) and dpa data are provided in Table 3-1 and Table 3-2. These data tabulations include both plant and fuel cycle specific calculated neutron exposures at the end of the tenth fuel cycle as well as future projections to 15, 20, 25, 32, 36, 48, and 54 EFPY. The calculations for Cycle 10 account for an uprate from 3411 MWt to 3458 MWt that occurred at the onset of cycle ten. The projections were based on the assumption that the core power distributions and associated plant operating characteristics from Cycle 10 were representative of future plant operation. The future projections are also based on the current reactor power level of 3458 MWt.

Radial gradient information applicable to fast (E > 1.0 MeV) neutron fluence and dpa are given in Tables 3-3 and 3-4, respectively. The data, based on maximum cumulative integrated exposures at the end of Cycle 10, are presented on a relative basis for each exposure parameter at several azimuthal locations. Exposure distributions through the vessel wall may be obtained by multiplying the calculated exposure at the vessel inner radius by the gradient data listed in Tables 3-3 and 3-4.

The calculated fast neutron exposures for the two surveillance capsules withdrawn from the Comanche Peak Unit 1 reactor are provided in Table 3-5 (also shown in Table 3-1 under the "Dual 31.5°" Column for Capsule X and under the "29° Dual" Column for Capsule Y). These assigned neutron exposure levels are based on the plant and fuel cycle specific neutron transport calculations performed for the Comanche Peak Unit 1 reactor.

Updated lead factors for the Comanche Peak Unit 1 surveillance capsules are provided in Table 3-6. The capsule lead factor is defined as the ratio of the calculated fluence (E > 1.0 MeV) at the geometric center of the surveillance capsule to the corresponding maximum calculated fluence at the pressure vessel clad/base metal interface. In Table 3-6, the lead factors for capsules that have been withdrawn from the reactor (U and Y) were based on the calculated fluence values for the irradiation period corresponding to the time of withdrawal for the individual capsules. For the capsules remaining in the reactor (V, W, X, and Z), the lead factor corresponds to the calculated fluence values at the end of Cycle 10, the last completed fuel cycle for Comanche Peak Unit 1.

3.3 NEUTRON DOSIMETRY

The validity of the calculated neutron exposures previously reported in Section 3.2 is demonstrated by a direct comparison against the measured sensor reaction rates and via a least squares evaluation performed for each of the capsule dosimetry sets. However, since the neutron dosimetry measurement data merely serves to validate the calculated results, only the direct comparison of measured-to-calculated results for the most recent surveillance capsule removed from service is provided in this section of the report. For completeness, the assessment of all measured dosimetry removed to date, based on both direct and least squares evaluation comparisons, is documented in Appendix A.

The direct comparison of measured versus calculated fast neutron threshold reaction rates for the sensors from Capsule Y, that was withdrawn from Comanche Peak Unit 1 at the end of the sixth fuel cycle, is summarized below.

Reaction	Reaction Rates (rps/atom)		M/C Ratio
	Measured	Calculated	
$^{63}Cu(n,\alpha)^{60}Co$	4.77E-17	4.16E-17	1.15
$^{54}Fe(n,p)^{54}Mn$	4.78E-15	4.55E-15	1.05
$^{58}Ni(n,p)^{58}Co$	6.51E-15	6.37E-15	1.02
$^{238}U(n,p)^{137}Cs$ (Cd)	2.93E-14	2.43E-14	1.21
$^{237}Np(n,f)^{137}Cs$ (Cd)	2.57E-13	2.36E-13	1.09
		Average:	1.10
		% Standard Deviation:	6.7

The measured-to-calculated (M/C) reaction rate ratios for the Capsule Y threshold reactions range from 1.02 to 1.21, and the average M/C ratio is $1.10 \pm 6.7\%$ (1σ). This direct comparison falls well within the $\pm 20\%$ criterion specified in Regulatory Guide 1.190; furthermore, it is consistent with the full set of comparisons given in Appendix A for all measured dosimetry removed to date from the Comanche Peak Unit 1 reactor. These comparisons validate the current analytical results described in Section 3.2; therefore, the calculations are deemed applicable for Comanche Peak Unit 1.

3.4 CALCULATIONAL UNCERTAINTIES

The uncertainty associated with the calculated neutron exposure of the Comanche Peak Unit 1 surveillance capsule and reactor pressure vessel is based on the recommended approach provided in Regulatory Guide 1.190. In particular, the qualification of the methodology was carried out in the following four stages:

1 - Comparison of calculations with benchmark measurements from the Pool Critical Assembly (PCA) simulator at the Oak Ridge National Laboratory (ORNL).

2 - Comparisons of calculations with surveillance capsule and reactor cavity measurements from the H. B. Robinson power reactor benchmark experiment.

3 - An analytical sensitivity study addressing the uncertainty components resulting from important input parameters applicable to the plant specific transport calculations used in the neutron exposure assessments.

4 - Comparisons of the plant specific calculations with all available dosimetry results from the Comanche Peak Unit 1 surveillance program.

The first phase of the methods qualification (PCA comparisons) addressed the adequacy of basic transport calculation and dosimetry evaluation techniques and associated cross-sections. This phase, however, did not test the accuracy of commercial core neutron source calculations nor did it address uncertainties in operational or geometric variables that impact power reactor calculations. The second phase of the qualification (H. B. Robinson comparisons) addressed uncertainties in these additional areas that are primarily methods related and would tend to apply generically to all fast neutron exposure evaluations. The third phase of the qualification (analytical sensitivity study) identified the potential uncertainties introduced into the overall evaluation due to calculational methods approximations as well as to a lack of knowledge relative to various plant specific input parameters. The overall calculational uncertainty applicable to the Comanche Peak Unit 1 analysis was established from results of these three phases of the methods qualification.

The fourth phase of the uncertainty assessment (comparisons with Comanche Peak Unit 1 measurements) was used solely to demonstrate the validity of the transport calculations and to confirm the uncertainty estimates associated with the analytical results. The comparison was used only as a check and was not used in any way to modify the calculated surveillance capsule and pressure vessel neutron exposures previously described in Section 3.2. As such, the validation of the Comanche Peak Unit 1 analytical model based on the measured plant dosimetry is completely described in Appendix A.

The following summarizes the uncertainties developed from the first three phases of the methodology qualification. Additional information pertinent to these evaluations is provided in Reference 2.

	Capsule	Vessel IR
PCA Comparisons	3%	3%
H. B. Robinson Comparisons	3%	3%
Analytical Sensitivity Studies	10%	11%
Additional Uncertainty for Factors not Explicitly Evaluated	5%	5%
Net Calculational Uncertainty	12%	13%

The net calculational uncertainty was determined by combining the individual components in quadrature. Therefore, the resultant uncertainty was treated as random and no systematic bias was applied to the analytical results.

The plant specific measurement comparisons described in Appendix A support these uncertainty assessments for Comanche Peak Unit 1.

TABLE 3-1

Calculated Neutron Exposure Rates And Integrated Exposures
At The Surveillance Capsule Center

Cycle	Cycle Length [EFPS]	Cumulative Irradiation Time		Neutron Flux (E > 1.0 MeV) [n/cm²-s]		
		[EFPS]	[EFPY]	Dual 29°	Dual 31.5°	Single 31.5°
1	2.89E+07	2.89E+07	0.91	1.02E+11	1.10E+11	1.09E+11
2	2.43E+07	5.32E+07	1.68	6.54E+10	7.31E+10	7.25E+10
3	2.30E+07	7.62E+07	2.41	7.22E+10	8.07E+10	8.00E+10
4	3.70E+07	1.13E+08	3.59	8.39E+10	9.19E+10	9.11E+10
5	4.24E+07	1.56E+08	4.93	7.03E+10	7.19E+10	7.11E+10
6	4.14E+07	1.97E+08	6.24	6.45E+10	7.19E+10	7.13E+10
7	4.41E+07	2.41E+08	7.64	6.82E+10	7.25E+10	7.18E+10
8	4.37E+07	2.85E+08	9.02	6.40E+10	6.95E+10	6.88E+10
9	4.39E+07	3.29E+08	10.42	6.98E+10	7.14E+10	7.05E+10
10	4.01E+07	3.69E+08	11.69	7.76E+10	7.98E+10	7.89E+10
Future	1.05E+08	4.73E+08	15.00	7.76E+10	7.98E+10	7.89E+10
Future	1.58E+08	6.31E+08	20.00	7.76E+10	7.98E+10	7.89E+10
Future	1.58E+08	7.89E+08	25.00	7.76E+10	7.98E+10	7.89E+10
Future	2.21E+08	1.01E+09	32.00	7.76E+10	7.98E+10	7.89E+10
Future	1.26E+08	1.14E+09	36.00	7.76E+10	7.98E+10	7.89E+10
Future	3.79E+08	1.51E+09	48.00	7.76E+10	7.98E+10	7.89E+10
Future	1.89E+08	1.70E+09	54.00	7.76E+10	7.98E+10	7.89E+10

Note: Neutron exposure values reported for the surveillance capsules are centered at the core midplane.

TABLE 3-1 cont'd

Calculated Neutron Exposure Rates And Integrated Exposures
At The Surveillance Capsule Center

Cycle	Cycle Length [EFPS]	Cumulative Irradiation Time		Neutron Fluence (E > 1.0 MeV) [n/cm²]		
		[EFPS]	[EFPY]	Dual 29°	Dual 31.5°	Single 31.5°
1	2.89E+07	2.89E+07	0.91	2.93E+18	3.18E+18	3.15E+18
2	2.43E+07	5.32E+07	1.68	4.52E+18	4.96E+18	4.91E+18
3	2.30E+07	7.62E+07	2.41	6.18E+18	6.82E+18	6.76E+18
4	3.70E+07	1.13E+08	3.59	9.28E+18	1.02E+19	1.01E+19
5	4.24E+07	1.56E+08	4.93	1.23E+19	1.33E+19	1.31E+19
6	4.14E+07	1.97E+08	6.24	1.49E+19	1.62E+19	1.61E+19
7	4.41E+07	2.41E+08	7.64	1.79E+19	1.94E+19	1.93E+19
8	4.37E+07	2.85E+08	9.02	2.07E+19	2.25E+19	2.23E+19
9	4.39E+07	3.29E+08	10.42	2.38E+19	2.56E+19	2.54E+19
10	4.01E+07	3.69E+08	11.69	2.69E+19	2.88E+19	2.85E+19
Future	1.05E+08	4.73E+08	15.00	3.50E+19	3.72E+19	3.68E+19
Future	1.58E+08	6.31E+08	20.00	4.73E+19	4.98E+19	4.92E+19
Future	1.58E+08	7.89E+08	25.00	5.95E+19	6.24E+19	6.17E+19
Future	2.21E+08	1.01E+09	32.00	7.67E+19	8.00E+19	7.91E+19
Future	1.26E+08	1.14E+09	36.00	8.65E+19	9.01E+19	8.91E+19
Future	3.79E+08	1.51E+09	48.00	1.16E+20	1.20E+20	1.19E+20
Future	1.89E+08	1.70E+09	54.00	1.31E+20	1.35E+20	1.34E+20

Note: Neutron exposure values reported for the surveillance capsules are centered at the
core midplane.

TABLE 3-1 cont'd

Calculated Neutron Exposure Rates And Integrated Exposures
At The Surveillance Capsule Center

Cycle	Cycle Length [EFPS]	Cumulative Irradiation Time		Iron Atom Displacement Rate [dpa/s]		
		[EFPS]	[EFPY]	Dual 29°	Dual 31.5°	Single 31.5°
1	2.89E+07	2.89E+07	0.91	1.99E-10	2.16E-10	2.14E-10
2	2.43E+07	5.32E+07	1.68	1.27E-10	1.42E-10	1.41E-10
3	2.30E+07	7.62E+07	2.41	1.40E-10	1.56E-10	1.55E-10
4	3.70E+07	1.13E+08	3.59	1.63E-10	1.78E-10	1.77E-10
5	4.24E+07	1.56E+08	4.93	1.37E-10	1.40E-10	1.38E-10
6	4.14E+07	1.97E+08	6.24	1.26E-10	1.40E-10	1.39E-10
7	4.41E+07	2.41E+08	7.64	1.33E-10	1.41E-10	1.39E-10
8	4.37E+07	2.85E+08	9.02	1.24E-10	1.35E-10	1.33E-10
9	4.39E+07	3.29E+08	10.42	1.36E-10	1.39E-10	1.37E-10
10	4.01E+07	3.69E+08	11.69	1.51E-10	1.55E-10	1.53E-10
Future	1.05E+08	4.73E+08	15.00	1.51E-10	1.55E-10	1.53E-10
Future	1.58E+08	6.31E+08	20.00	1.51E-10	1.55E-10	1.53E-10
Future	1.58E+08	7.89E+08	25.00	1.51E-10	1.55E-10	1.53E-10
Future	2.21E+08	1.01E+09	32.00	1.51E-10	1.55E-10	1.53E-10
Future	1.26E+08	1.14E+09	36.00	1.51E-10	1.55E-10	1.53E-10
Future	3.79E+08	1.51E+09	48.00	1.51E-10	1.55E-10	1.53E-10
Future	1.89E+08	1.70E+09	54.00	1.51E-10	1.55E-10	1.53E-10

Note: Neutron exposure values reported for the surveillance capsules are centered at the
core midplane.

TABLE 3-1 cont'd

Calculated Neutron Exposure Rates And Integrated Exposures
At The Surveillance Capsule Center

Cycle	Cycle Length [EFPS]	Cumulative Irradiation Time		Iron Atom Displacements [dpa]		
		[EFPS]	[EFPY]	Dual 29°	Dual 31.5°	Single 31.5°
1	2.89E+07	2.89E+07	0.91	5.74E-03	6.24E-03	6.17E-03
2	2.43E+07	5.32E+07	1.68	8.83E-03	9.68E-03	9.59E-03
3	2.30E+07	7.62E+07	2.41	1.21E-02	1.33E-02	1.32E-02
4	3.70E+07	1.13E+08	3.59	1.81E-02	1.99E-02	1.97E-02
5	4.24E+07	1.56E+08	4.93	2.39E-02	2.58E-02	2.55E-02
6	4.14E+07	1.97E+08	6.24	2.91E-02	3.16E-02	3.13E-02
7	4.41E+07	2.41E+08	7.64	3.49E-02	3.78E-02	3.74E-02
8	4.37E+07	2.85E+08	9.02	4.04E-02	4.37E-02	4.32E-02
9	4.39E+07	3.29E+08	10.42	4.63E-02	4.98E-02	4.93E-02
10	4.01E+07	3.69E+08	11.69	5.24E-02	5.60E-02	5.54E-02
Future	1.05E+08	4.73E+08	15.00	6.82E-02	7.22E-02	7.14E-02
Future	1.58E+08	6.31E+08	20.00	9.20E-02	9.67E-02	9.55E-02
Future	1.58E+08	7.89E+08	25.00	1.16E-01	1.21E-01	1.20E-01
Future	2.21E+08	1.01E+09	32.00	1.49E-01	1.55E-01	1.54E-01
Future	1.26E+08	1.14E+09	36.00	1.68E-01	1.75E-01	1.73E-01
Future	3.79E+08	1.51E+09	48.00	2.25E-01	2.34E-01	2.31E-01
Future	1.89E+08	1.70E+09	54.00	2.54E-01	2.63E-01	2.60E-01

Note: Neutron exposure values reported for the surveillance capsules are centered at the
core midplane.

TABLE 3-2

Calculated Azimuthal Variation Of Maximum Exposure Rates
And Integrated Exposures At The Reactor Vessel
Clad/Base Metal Interface

Cycle	Cycle Length [EFPS]	Cumulative Irradiation Time		Neutron Flux (E > 1.0 MeV) [n/cm²-s]				
		[EFPS]	[EFPY]	0°	15°	21°	30°	45°
1	2.89E+07	2.89E+07	0.91	1.42E+10	2.18E+10	2.59E+10	2.54E+10	2.75E+10
2	2.43E+07	5.32E+07	1.68	9.96E+09	1.38E+10	1.58E+10	1.70E+10	1.81E+10
3	2.30E+07	7.62E+07	2.41	1.05E+10	1.45E+10	1.69E+10	1.84E+10	1.94E+10
4	3.70E+07	1.13E+08	3.59	1.05E+10	1.77E+10	2.07E+10	2.11E+10	2.09E+10
5	4.24E+07	1.56E+08	4.93	1.31E+10	1.95E+10	2.10E+10	1.77E+10	1.60E+10
6	4.14E+07	1.97E+08	6.24	1.14E+10	1.43E+10	1.61E+10	1.66E+10	1.85E+10
7	4.41E+07	2.41E+08	7.64	1.38E+10	1.92E+10	2.01E+10	1.76E+10	1.75E+10
8	4.37E+07	2.85E+08	9.02	1.20E+10	1.54E+10	1.70E+10	1.65E+10	1.69E+10
9	4.39E+07	3.29E+08	10.42	1.35E+10	1.97E+10	2.11E+10	1.78E+10	1.53E+10
10	4.01E+07	3.69E+08	11.69	1.29E+10	2.01E+10	2.24E+10	1.96E+10	1.74E+10
Future	1.05E+08	4.73E+08	15.00	1.29E+10	2.01E+10	2.24E+10	1.96E+10	1.74E+10
Future	1.58E+08	6.31E+08	20.00	1.29E+10	2.01E+10	2.24E+10	1.96E+10	1.74E+10
Future	1.58E+08	7.89E+08	25.00	1.29E+10	2.01E+10	2.24E+10	1.96E+10	1.74E+10
Future	2.21E+08	1.01E+09	32.00	1.29E+10	2.01E+10	2.24E+10	1.96E+10	1.74E+10
Future	1.26E+08	1.14E+09	36.00	1.29E+10	2.01E+10	2.24E+10	1.96E+10	1.74E+10
Future	3.79E+08	1.51E+09	48.00	1.29E+10	2.01E+10	2.24E+10	1.96E+10	1.74E+10
Future	1.89E+08	1.70E+09	54.00	1.29E+10	2.01E+10	2.24E+10	1.96E+10	1.74E+10

TABLE 3-2 cont'd

Calculated Azimuthal Variation Of Maximum Exposure Rates
And Integrated Exposures At The Reactor Vessel
Clad/Base Metal Interface

Cycle	Cycle Length [EFPS]	Cumulative Irradiation Time		Neutron Fluence (E > 1.0 MeV) [n/cm²]				
		[EFPS]	[EFPY]	0°	15°	21°	30°	45°
1	2.89E+07	2.89E+07	0.91	4.10E+17	6.28E+17	7.48E+17	7.32E+17	7.93E+17
2	2.43E+07	5.32E+07	1.68	6.45E+17	9.55E+17	1.12E+18	1.13E+18	1.22E+18
3	2.30E+07	7.62E+07	2.41	8.86E+17	1.29E+18	1.51E+18	1.56E+18	1.67E+18
4	3.70E+07	1.13E+08	3.59	1.27E+18	1.94E+18	2.27E+18	2.34E+18	2.44E+18
5	4.24E+07	1.56E+08	4.93	1.82E+18	2.76E+18	3.15E+18	3.07E+18	3.11E+18
6	4.14E+07	1.97E+08	6.24	2.30E+18	3.35E+18	3.82E+18	3.76E+18	3.87E+18
7	4.41E+07	2.41E+08	7.64	2.89E+18	4.19E+18	4.69E+18	4.53E+18	4.64E+18
8	4.37E+07	2.85E+08	9.02	3.42E+18	4.86E+18	5.43E+18	5.25E+18	5.38E+18
9	4.39E+07	3.29E+08	10.42	4.01E+18	5.73E+18	6.36E+18	6.03E+18	6.05E+18
10	4.01E+07	3.69E+08	11.69	4.53E+18	6.53E+18	7.26E+18	6.82E+18	6.75E+18
Future	1.05E+08	4.73E+08	15.00	5.88E+18	8.63E+18	9.60E+18	8.87E+18	8.56E+18
Future	1.58E+08	6.31E+08	20.00	7.91E+18	1.18E+19	1.31E+19	1.20E+19	1.13E+19
Future	1.58E+08	7.89E+08	25.00	9.95E+18	1.50E+19	1.67E+19	1.51E+19	1.40E+19
Future	2.21E+08	1.01E+09	32.00	1.28E+19	1.94E+19	2.16E+19	1.94E+19	1.79E+19
Future	1.26E+08	1.14E+09	36.00	1.44E+19	2.20E+19	2.45E+19	2.19E+19	2.01E+19
Future	3.79E+08	1.51E+09	48.00	1.93E+19	2.96E+19	3.29E+19	2.93E+19	2.67E+19
Future	1.89E+08	1.70E+09	54.00	2.17E+19	3.34E+19	3.72E+19	3.30E+19	2.99E+19

TABLE 3-2 cont'd

Calculated Azimuthal Variation Of Fast Neutron Exposure Rates
And Iron Atom Displacement Rates At The Reactor Vessel
Clad/Base Metal Interface

Cycle	Cycle Length [EFPS]	Cumulative Irradiation Time		Iron Atom Displacement Rate [dpa/s]				
		[EFPS]	[EFPY]	0°	15°	21°	30°	45°
1	2.89E+07	2.89E+07	0.91	2.21E-11	3.34E-11	3.97E-11	3.91E-11	4.35E-11
2	2.43E+07	5.32E+07	1.68	1.55E-11	2.13E-11	2.43E-11	2.62E-11	2.86E-11
3	2.30E+07	7.62E+07	2.41	1.63E-11	2.24E-11	2.59E-11	2.83E-11	3.07E-11
4	3.70E+07	1.13E+08	3.59	1.63E-11	2.72E-11	3.17E-11	3.26E-11	3.31E-11
5	4.24E+07	1.56E+08	4.93	2.04E-11	2.99E-11	3.21E-11	2.73E-11	2.53E-11
6	4.14E+07	1.97E+08	6.24	1.76E-11	2.21E-11	2.48E-11	2.57E-11	2.93E-11
7	4.41E+07	2.41E+08	7.64	2.14E-11	2.95E-11	3.08E-11	2.72E-11	2.78E-11
8	4.37E+07	2.85E+08	9.02	1.87E-11	2.36E-11	2.60E-11	2.55E-11	2.68E-11
9	4.39E+07	3.29E+08	10.42	2.09E-11	3.03E-11	3.23E-11	2.74E-11	2.43E-11
10	4.01E+07	3.69E+08	11.69	2.01E-11	3.09E-11	3.43E-11	3.02E-11	2.75E-11
Future	1.05E+08	4.73E+08	15.00	2.01E-11	3.09E-11	3.43E-11	3.02E-11	2.75E-11
Future	1.58E+08	6.31E+08	20.00	2.01E-11	3.09E-11	3.43E-11	3.02E-11	2.75E-11
Future	1.58E+08	7.89E+08	25.00	2.01E-11	3.09E-11	3.43E-11	3.02E-11	2.75E-11
Future	2.21E+08	1.01E+09	32.00	2.01E-11	3.09E-11	3.43E-11	3.02E-11	2.75E-11
Future	1.26E+08	1.14E+09	36.00	2.01E-11	3.09E-11	3.43E-11	3.02E-11	2.75E-11
Future	3.79E+08	1.51E+09	48.00	2.01E-11	3.09E-11	3.43E-11	3.02E-11	2.75E-11
Future	1.89E+08	1.70E+09	54.00	2.01E-11	3.09E-11	3.43E-11	3.02E-11	2.75E-11

TABLE 3-2 cont'd

Calculated Azimuthal Variation Of Maximum Exposure Rates
And Integrated Exposures At The Reactor Vessel
Clad/Base Metal Interface

Cycle	Cycle Length [EFPS]	Cumulative Irradiation Time		Iron Atom Displacements [dpa]				
		[EFPS]	[EFPY]	0°	15°	21°	30°	45°
1	2.89E+07	2.89E+07	0.91	6.36E-04	9.64E-04	1.14E-03	1.13E-03	1.25E-03
2	2.43E+07	5.32E+07	1.68	1.00E-03	1.47E-03	1.72E-03	1.75E-03	1.93E-03
3	2.30E+07	7.62E+07	2.41	1.38E-03	1.98E-03	2.32E-03	2.40E-03	2.64E-03
4	3.70E+07	1.13E+08	3.59	1.98E-03	2.99E-03	3.49E-03	3.60E-03	3.86E-03
5	4.24E+07	1.56E+08	4.93	2.84E-03	4.24E-03	4.83E-03	4.74E-03	4.91E-03
6	4.14E+07	1.97E+08	6.24	3.57E-03	5.15E-03	5.86E-03	5.81E-03	6.12E-03
7	4.41E+07	2.41E+08	7.64	4.50E-03	6.44E-03	7.20E-03	6.99E-03	7.33E-03
8	4.37E+07	2.85E+08	9.02	5.31E-03	7.47E-03	8.34E-03	8.11E-03	8.51E-03
9	4.39E+07	3.29E+08	10.42	6.23E-03	8.80E-03	9.76E-03	9.31E-03	9.57E-03
10	4.01E+07	3.69E+08	11.69	7.04E-03	1.00E-02	1.11E-02	1.05E-02	1.07E-02
Future	1.05E+08	4.73E+08	15.00	9.13E-03	1.33E-02	1.47E-02	1.37E-02	1.36E-02
Future	1.58E+08	6.31E+08	20.00	1.23E-02	1.81E-02	2.01E-02	1.85E-02	1.79E-02
Future	1.58E+08	7.89E+08	25.00	1.55E-02	2.30E-02	2.56E-02	2.32E-02	2.22E-02
Future	2.21E+08	1.01E+09	32.00	1.99E-02	2.98E-02	3.31E-02	2.99E-02	2.83E-02
Future	1.26E+08	1.14E+09	36.00	2.24E-02	3.37E-02	3.75E-02	3.37E-02	3.18E-02
Future	3.79E+08	1.51E+09	48.00	3.00E-02	4.54E-02	5.04E-02	4.52E-02	4.22E-02
Future	1.89E+08	1.70E+09	54.00	3.38E-02	5.13E-02	5.69E-02	5.09E-02	4.74E-02

TABLE 3-3

Relative Radial Distribution Of Neutron Fluence (E > 1.0 MeV)
Within The Reactor Vessel Wall

RADIUS	AZIMUTHAL ANGLE				
(cm)	0°	15°	21°	30°	45°
220.11	1.000	1.000	1.000	1.000	1.000
225.59	0.571	0.566	0.564	0.561	0.558
231.06	0.282	0.276	0.274	0.273	0.269
236.54	0.134	0.129	0.128	0.128	0.125
242.01	0.064	0.059	0.058	0.059	0.057
Note:	Base Metal Inner Radius = 220.11 cm				
	Base Metal 1/4T = 225.59 cm				
	Base Metal 1/2T = 231.06 cm				
	Base Metal 3/4T = 236.54 cm				
	Base Metal Outer Radius = 242.01 cm				

Note: Relative radial distribution data are based on the maximum
cumulative integrated exposures from Cycles 1 through 10.

TABLE 3-4

Relative Radial Distribution Of Iron Atom Displacements (dpa)
Within The Reactor Vessel Wall

RADIUS	AZIMUTHAL ANGLE				
(cm)	0°	15°	21°	30°	45°
220.11	1.000	1.000	1.000	1.000	1.000
225.59	0.644	0.636	0.635	0.637	0.646
231.06	0.392	0.381	0.379	0.384	0.395
236.54	0.239	0.227	0.225	0.231	0.239
242.01	0.144	0.129	0.126	0.133	0.136
Note:	Base Metal Inner Radius = 220.11 cm				
	Base Metal 1/4T = 225.59 cm				
	Base Metal 1/2T = 231.06 cm				
	Base Metal 3/4T = 236.54 cm				
	Base Metal Outer Radius = 242.01 cm				

Note: Relative radial distribution data are based on the maximum
cumulative integrated exposures from Cycles 1 through 10.

TABLE 3-5

Calculated Fast Neutron Exposure of Surveillance Capsules
Withdrawn from Comanche Peak Unit 1

Capsule	Irradiation Time [EFPY]	Fluence (E > 1.0 MeV) [n/cm²]	Iron Displacements [dpa]
U	0.91	3.18E+18	6.24E-03
Y	6.24	1.49E+19	2.91E-02

TABLE 3-6

Calculated Surveillance Capsule Lead Factors

Capsule ID And Location	Status	Lead Factor[b]
U (31.5° Dual)	Withdrawn EOC 1	4.01
Y (29.0° Dual)	Withdrawn EOC 6	3.85
V (29.0° Dual)	Withdrawn EOC 9[a]	3.74
W (31.5° Single)	Withdrawn EOC 9[a]	3.99
X (31.5° Dual)	In Reactor	3.97
Z (31.5° Single)	In Reactor	3.93

Note:

(a) Capsules were removed during 1RF09 and transferred to the spent fuel pool.

(b) Lead factors for capsules remaining in the reactor are based on cycle specific exposure calculations through the last completed fuel cycle, i.e., Cycle 10.

FIGURE 3-1

Comanche Peak Unit 1 r,θ Reactor Geometry with a 12.5° Neutron Pad Span at the Core Midplane

R Axis (cm)
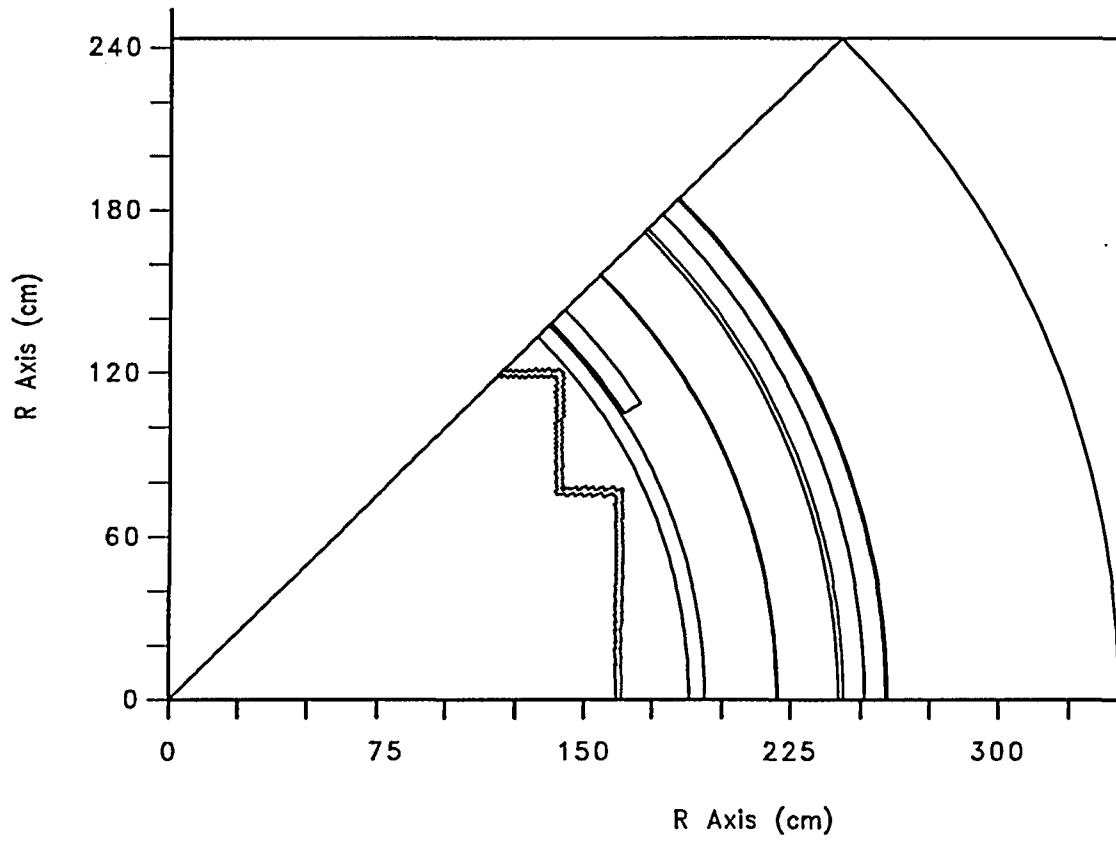
FIGURE 3-1 (continued)

Comanche Peak Unit 1 r,θ Reactor Geometry with a 20.0° Neutron Pad Span at the Core Midplane
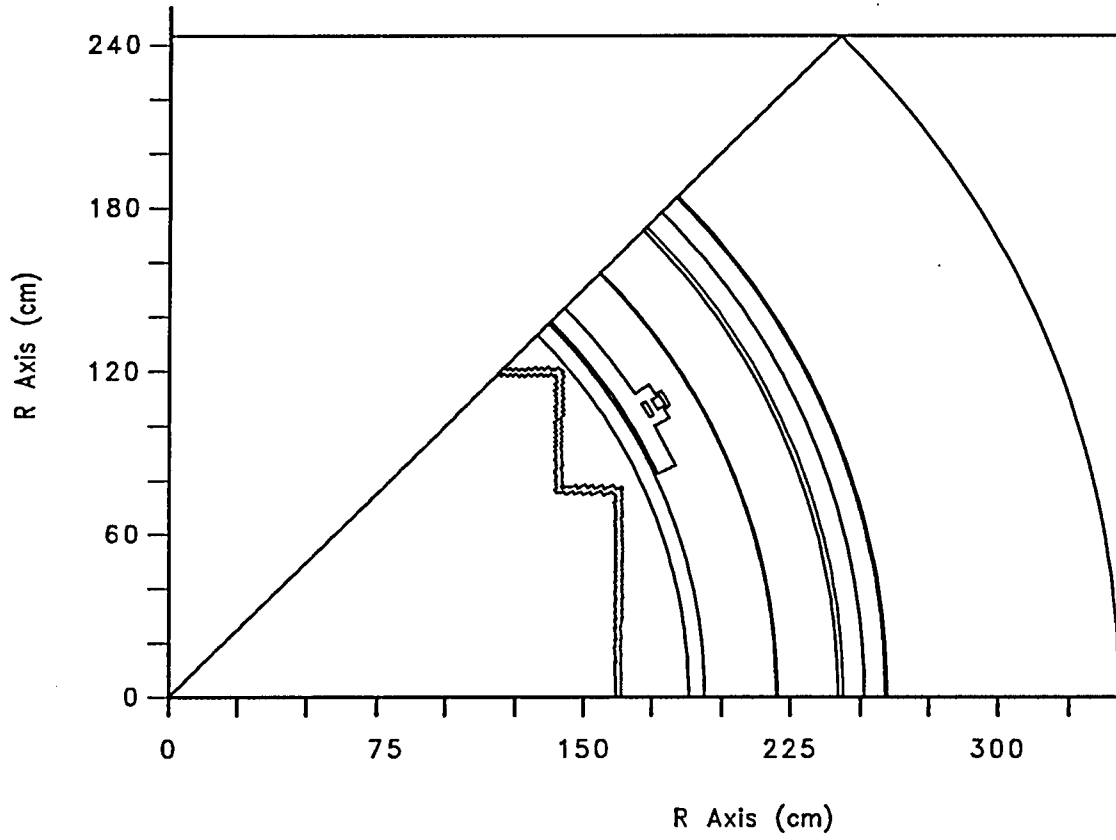
FIGURE 3-1 (continued)

Comanche Peak Unit 1 r,θ Reactor Geometry with a 22.5° Neutron Pad Span at the Core Midplane
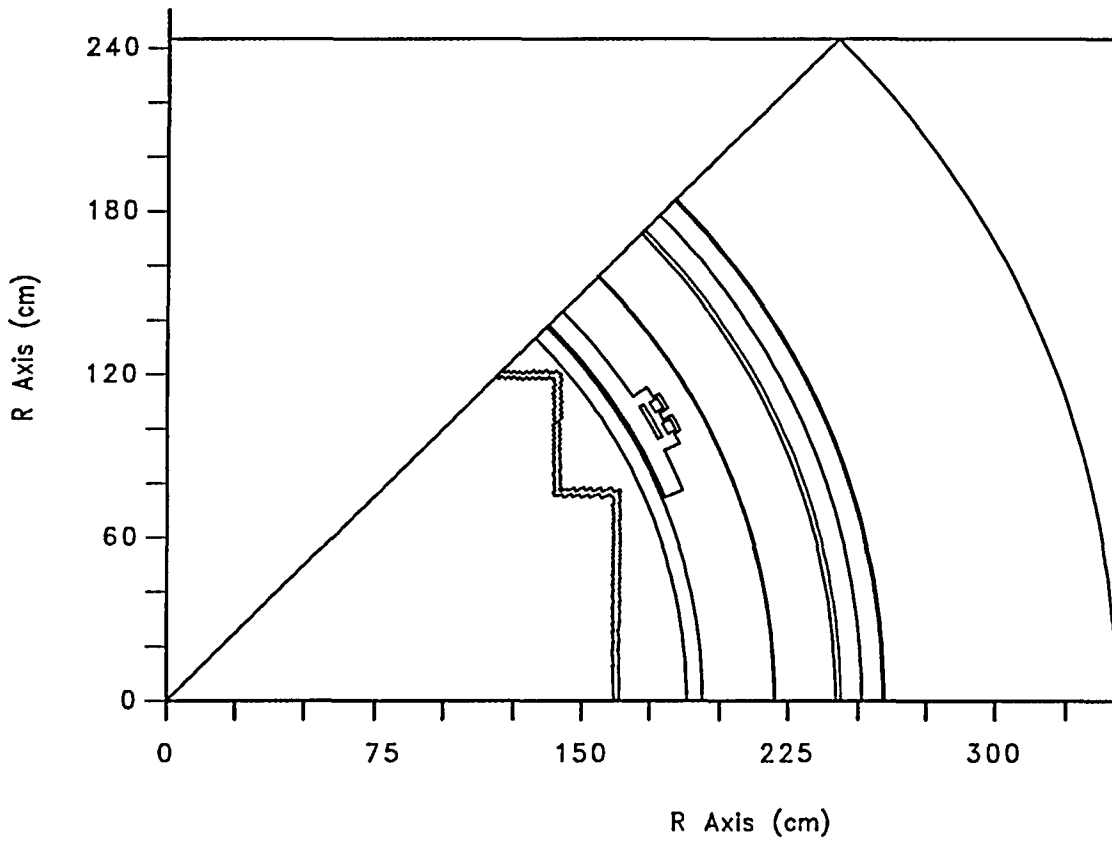
FIGURE 3-2

Comanche Peak Unit 1 r,z Reactor Geometry with Neutron Pad
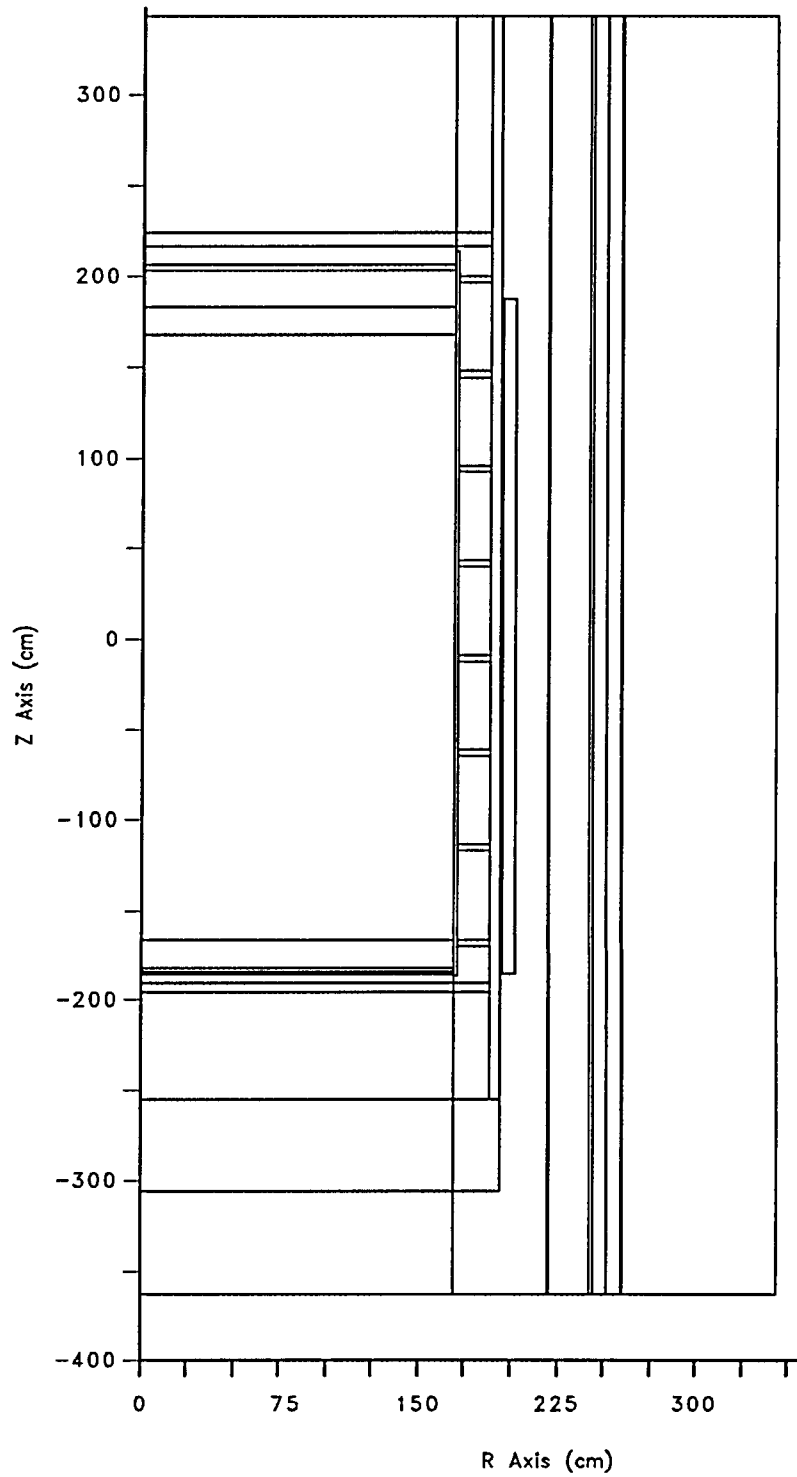
4   CRITERIA FOR ALLOWABLE PRESSURE-TEMPERATURE RELATIONSHIPS

4.1   OVERALL APPROACH

The ASME approach for calculating the allowable limit curves for various heatup and cooldown rates specifies that the total stress intensity factor, K_I, for the combined thermal and pressure stresses at any time during heatup or cooldown cannot be greater than the reference stress intensity factor, K_{Ic}, for the metal temperature at that time. K_{Ic} is obtained from the reference fracture toughness curve, defined in the 1998 Edition through the 2000 Addenda of Section XI, Appendix G of the ASME Code[12]. The K_{Ic} curve is given by the following equation:

$$K_{Ic} = 33.2 + 20.734 * e^{[0.02(T - RT_{NDT})]} \tag{1}$$

where,

K_{Ic} =   reference stress intensity factor as a function of the metal temperature T and the metal reference nil-ductility temperature RT_{NDT}

This K_{Ic} curve is based on the lower bound of static critical K_I values measured as a function of temperature on specimens of SA-533 Grade B Class1, SA-508-1, SA-508-2, SA-508-3 steel.

4.2 METHODOLOGY FOR PRESSURE-TEMPERATURE LIMIT CURVE DEVELOPMENT

The governing equation for the heatup-cooldown analysis is defined in Appendix G of the ASME Code as follows:

$$C* K_{Im} + K_{It} < K_{Ic} \tag{2}$$

where,

K_{Im} =   stress intensity factor caused by membrane (pressure) stress

K_{It} =   stress intensity factor caused by the thermal gradients

K_{Ic} =   function of temperature relative to the RT_{NDT} of the material

C   =   2.0 for Level A and Level B service limits

C   =   1.5 for hydrostatic and leak test conditions during which the reactor core is not critical

For membrane tension, the corresponding K_I for the postulated defect is:

$$K_{Im} = M_m \times (pR_i / t) \tag{3}$$

where, M_m for an inside surface flaw is given by:

$$M_m = 1.85 \text{ for } \sqrt{t} < 2,$$
$$M_m = 0.926\sqrt{t} \text{ for } 2 \leq \sqrt{t} \leq 3.464,$$
$$M_m = 3.21 \text{ for } \sqrt{t} > 3.464$$

Similarly, M_m for an outside surface flaw is given by:

$$M_m = 1.77 \text{ for } \sqrt{t} < 2,$$
$$M_m = 0.893\sqrt{t} \text{ for } 2 \leq \sqrt{t} \leq 3.464,$$
$$M_m = 3.09 \text{ for } \sqrt{t} > 3.464$$

and p = internal pressure, Ri = vessel inner radius, and t = vessel wall thickness.

For bending stress, the corresponding K_I for the postulated defect is:

$$K_{Ib} = M_b * \text{Maximum Stress, where } M_b \text{ is two-thirds of } M_m$$

The maximum K_I produced by radial thermal gradient for the postulated inside surface defect of G-2120 is $K_{It} = 0.953 \times 10^{-3} \times CR \times t^{2.5}$, where CR is the cooldown rate in °F/hr., or for a postulated outside surface defect, $K_{It} = 0.753 \times 10^{-3} \times HU \times t^{2.5}$, where HU is the heatup rate in °F/hr.

The through-wall temperature difference associated with the maximum thermal K_I can be determined from Fig. G-2214-1. The temperature at any radial distance from the vessel surface can be determined from Fig. G-2214-2 for the maximum thermal K_I.

(a)   The maximum thermal K_I relationship and the temperature relationship in Fig. G-2214-1 are applicable only for the conditions given in G-2214.3(a)(1) and (2).

(b)   Alternatively, the K_I for radial thermal gradient can be calculated for any thermal stress distribution and at any specified time during cooldown for a ¼-thickness inside surface defect using the relationship:

$$K_{It} = (1.0359C_0 + 0.6322C_1 + 0.4753C_2 + 0.3855C_3) * \sqrt{\pi a} \tag{4}$$

or similarly, K_{IT} during heatup for a ¼-thickness outside surface defect using the relationship:

$$K_{It} = (1.043C_0 + 0.630C_1 + 0.481C_2 + 0.401C_3) * \sqrt{\pi a} \qquad (5)$$

where the coefficients C_0, C_1, C_2 and C_3 are determined from the thermal stress distribution at any specified time during the heatup or cooldown using the form:

$$\sigma(x) = C_0 + C_1(x/a) + C_2(x/a)^2 + C_3(x/a)^3 \qquad (6)$$

and x is a variable that represents the radial distance from the appropriate (i.e., inside or outside) surface to any point on the crack front and a is the maximum crack depth.

Note, that equations 3, 4 and 5 were implemented in the OPERLIM computer code, which is the program used to generate the pressure-temperature (P-T) limit curves. No other changes were made to the OPERLIM computer code with regard to P-T calculation methodology. Therefore, the P-T curve methodology is unchanged from that described in WCAP-14040-NP-A, "Methodology used to Develop Cold Overpressure Mitigating System Setpoints and RCS Heatup and Cooldown Limit Curves"[2] Section 2.6 (equations 2.6.2-4 and 2.6.3-1) with the exceptions just described above.

At any time during the heatup or cooldown transient, K_{Ic} is determined by the metal temperature at the tip of a postulated flaw at the 1/4T and 3/4T location, the appropriate value for RT_{NDT}, and the reference fracture toughness curve. The thermal stresses resulting from the temperature gradients through the vessel wall are calculated and then the corresponding (thermal) stress intensity factors, K_{It}, for the reference flaw are computed. From Equation 2, the pressure stress intensity factors are obtained and, from these, the allowable pressures are calculated.

For the calculation of the allowable pressure versus coolant temperature during cooldown, the reference flaw of Appendix G to the ASME Code is assumed to exist at the inside of the vessel wall. During cooldown, the controlling location of the flaw is always at the inside of the wall because the thermal gradients produce tensile stresses at the inside, which increase with increasing cooldown rates. Allowable pressure-temperature relations are generated for both steady-state and finite cooldown rate situations. From these relations, composite limit curves are constructed for each cooldown rate of interest.

The use of the composite curve in the cooldown analysis is necessary because control of the cooldown procedure is based on the measurement of reactor coolant temperature, whereas the limiting pressure is actually dependent on the material temperature at the tip of the assumed flaw. During cooldown, the 1/4T vessel location is at a higher temperature than the fluid adjacent to the vessel inner diameter. This condition, of course, is not true for the steady-state situation. It follows that, at any given reactor coolant temperature, the ΔT (temperature) developed during cooldown results in a higher value of K_{Ic} at the 1/4T location for finite cooldown rates than for steady-state operation. Furthermore, if conditions exist so that the increase in K_{Ic} exceeds K_{It}, the calculated allowable pressure during cooldown will be greater than the steady-state value.

The above procedures are needed because there is no direct control on temperature at the 1/4T location and, therefore, allowable pressures may unknowingly be violated if the rate of cooling is decreased at various intervals along a cooldown ramp. The use of the composite curve eliminates this problem and ensures conservative operation of the system for the entire cooldown period.

Three separate calculations are required to determine the limit curves for finite heatup rates. As is done in the cooldown analysis, allowable pressure-temperature relationships are developed for steady-state conditions as well as finite heatup rate conditions assuming the presence of a 1/4T defect at the inside of the wall. The heatup results in compressive stresses at the inside surface that alleviate the tensile stresses produced by internal pressure. The metal temperature at the crack tip lags the coolant temperature; therefore, the K_{Ic} for the 1/4T crack during heatup is lower than the K_{Ic} for the 1/4T crack during steady-state conditions at the same coolant temperature. During heatup, especially at the end of the transient, conditions may exist so that the effects of compressive thermal stresses and lower K_{Ic} values do not offset each other, and the pressure-temperature curve based on steady-state conditions no longer represents a lower bound of all similar curves for finite heatup rates when the 1/4T flaw is considered. Therefore, both cases have to be analyzed in order to ensure that at any coolant temperature the lower value of the allowable pressure calculated for steady-state and finite heatup rates is obtained.

The second portion of the heatup analysis concerns the calculation of the pressure-temperature limitations for the case in which a 1/4T flaw located at the 1/4T location from the outside surface is assumed. Unlike the situation at the vessel inside surface, the thermal gradients established at the outside surface during heatup produce stresses which are tensile in nature and therefore tend to reinforce any pressure stresses present. These thermal stresses are dependent on both the rate of heatup and the time (or coolant temperature) along the heatup ramp. Since the thermal stresses at the outside are tensile and increase with increasing heatup rates, each heatup rate must be analyzed on an individual basis.

Following the generation of pressure-temperature curves for both the steady-state and finite heatup rate situations, the final limit curves are produced by constructing a composite curve based on a point-by-point comparison of the steady-state and finite heatup rate data. At any given temperature, the allowable pressure is taken to be the lesser of the three values taken from the curves under consideration. The use of the composite curve is necessary to set conservative heatup limitations because it is possible for conditions to exist wherein, over the course of the heatup ramp, the controlling condition switches from the inside to the outside, and the pressure limit must at all times be based on analysis of the most critical criterion.

4.3 CLOSURE HEAD/VESSEL FLANGE REQUIREMENTS

10 CFR Part 50, Appendix G[3] addresses the metal temperature of the closure head flange and vessel flange regions. This rule states that the metal temperature of the closure flange regions must exceed the material unirradiated RT_{NDT} by at least 120°F for normal operation when the pressure exceeds 20 percent of the preservice hydrostatic test pressure (3106 psi), which is 621 psig for Comanche Peak Units 1 and 2. The limiting unirradiated RT_{NDT} of 40°F occurs in both the closure head flanges of the Comanche Peak Units 1 and 2 reactor vessels, so the minimum allowable temperature of this region is 160°F at pressures greater than 621 psig. This limit is shown in Figures 6-1 through 6-4 wherever applicable.

5   CALCULATION OF ADJUSTED REFERENCE TEMPERATURE

From Regulatory Guide 1.99, Revision 2, the adjusted reference temperature (ART) for each material in the beltline region is given by the following expression:

$$ART = \text{Initial } RT_{NDT} + \Delta RT_{NDT} + \text{Margin} \tag{7}$$

Initial RT_{NDT} is the reference temperature for the unirradiated material as defined in paragraph NB-2331 of Section III of the ASME Boiler and Pressure Vessel Code[13]. If measured values of initial RT_{NDT} for the material in question are not available, generic mean values for that class of material may be used if there are sufficient test results to establish a mean and standard deviation for the class.

ΔRT_{NDT} is the mean value of the adjustment in reference temperature caused by irradiation and should be calculated as follows:

$$\Delta RT_{NDT} = CF * f^{(0.28 - 0.10 \log f)} \tag{8}$$

To calculate ΔRT_{NDT} at any depth (e.g., at 1/4T or 3/4T), the following formula must first be used to attenuate the fluence at the specific depth.

$$f_{(depth\ x)} = f_{surface} * e^{(-0.24x)} \tag{9}$$

where x inches (vessel beltline thickness is 8.63 inches) is the depth into the vessel wall measured from the vessel clad/base metal interface. The resultant fluence is then placed in Equation 8 to calculate the ΔRT_{NDT} at the specific depth.

The Westinghouse Radiation Engineering and Analysis Group evaluated the vessel fluence projections and the results of the **calculated peak fluence values** at various azimuthal locations on the vessel clad/base metal interface are presented in Table 5-1. The evaluation used the ENDF/B-VI scattering cross-section data set. This is consistent with methods presented in WCAP-14040-NP-A, "Methodology Used to Develop Cold Overpressure Mitigating System Setpoints and RCS Heatup and Cooldown Limit Curves". Tables 5-2 and 5-3 contain the 1/4T and 3/4T calculated fluences and fluence factors, per the Regulatory Guide 1.99, Revision 2, used to calculate the 36 EFPY ART values for all beltline materials in the Comanche Peak Units 1 and 2 reactor vessel.

Margin is calculated as, $M = 2 \sqrt{\sigma_i^2 + \sigma_\Delta^2}$. The standard deviation for the initial RT_{NDT} margin term, is σ_i 0°F when the initial RT_{NDT} is a measured value, and 17°F when a generic value is available. The standard deviation for the ΔRT_{NDT} margin term, σ_Δ, is 17°F for plates or forgings, and 8.5°F for plates or forgings when surveillance data is used. For welds, σ_Δ is equal to 28°F when surveillance capsule data is not used, and is 14°F (half the value) when credible surveillance capsule data is used. σ_Δ need not exceed 0.5 times the mean value of ΔRT_{NDT}.

Contained in Tables 5-4 through 5-7 are the calculations of the Unit 1 and Unit 2 36 EFPY ART values used for generation of the heatup and cooldown curves.

TABLE 5-1

Calculated Neutron Fluence Projections at the Peak Location
on the Reactor Vessel Clad/Base Metal Interface [n/cm^2, (E > 1.0 MeV)]

EFPY	Azimuthal Location				
	0°	15°	21°	30°	45°
Comanche Peak Unit 1					
32.00	1.28E+19	1.94E+19	2.16E+19	1.94E+19	1.79E+19
36.00	1.44E+19	2.20E+19	2.45E+19	2.19E+19	2.01E+19
48.00	1.93E+19	2.96E+19	3.29E+19	2.93E+19	2.67E+19
54.00	2.17E+19	3.34E+19	3.72E+19	3.30E+19	2.99E+19
Comanche Peak Unit 2					
32.00	1.42E+19	1.91E+19	N/A	1.93E+19	2.03E+19
36.00	1.60E+19	2.15E+19	N/A	2.17E+19	2.29E+19
48.00	2.14E+19	2.88E+19	N/A	2.89E+19	3.07E+19
54.00	2.41E+19	3.24E+19	N/A	3.26E+19	3.46E+19

TABLE 5-2

Summary of the Vessel Surface, 1/4T and 3/4T Fluence Values
used for the Generation of the 36 EFPY Heatup/Cooldown Curves for Comanche Peak Units 1 & 2

Vessel[a]	Surface[a] $(n/cm^2, E > 1.0\ MeV)$	1/4T $(n/cm^2, E > 1.0\ MeV)$	3/4T $(n/cm^2, E > 1.0\ MeV)$
Comanche Peak Unit 1	2.45×10^{19}	1.46×10^{19}	0.52×10^{19}
Comanche Peak Unit 2	2.29×10^{19}	1.36×10^{19}	0.48×10^{19}

Notes:

(a) The peak fluence from each Unit will be used for all the beltline materials, thus listing each material individually is not necessary.

TABLE 5-3

Summary of the 1/4T and 3/4T Fluence Factor Values
used for the Generation of the 36 EFPY Heatup/Cooldown Curves for Comanche Peak Units 1 & 2

Vessel[a]	1/4T F[b]	1/4T FF	3/4T F[b]	3/4T FF
Comanche Peak Unit 1	1.46×10^{19}	1.10	0.52×10^{19}	0.82
Comanche Peak Unit 2	1.36×10^{19}	1.09	0.48×10^{19}	0.80

Notes:

(a) The peak fluence from each Unit will be used for all the beltline materials, thus listing each material individually is not necessary.

(b) Units are $(n/cm^2, E > 1.0\ MeV)$.

TABLE 5-4
Calculation of the Comanche Peak Unit 1 ART Values for the 1/4T Location @ 36 EFPY

Material	Reg. Guide 1.99 Rev. 2 Method	CF$^{(a)}$ (°F)	¼ T FF	IRT$_{NDT}$$^{(b)}$ (°F)	ΔRT$_{NDT}$$^{(c)}$ (°F)	M$^{(d)}$ (°F)	ART$^{(e)}$ (°F)
Intermediate Shell Plate R-1107-1	Position 1.1	44	1.10	10	48.4	34	92
Intermediate Shell Plate R-1107-2	Position 1.1	44	1.10	-10	48.4	34	72
Intermediate Shell Plate R-1107-3	Position 1.1	37	1.10	10	40.7	34	85
Lower Shell Plate R-1108-1	Position 1.1	51	1.10	0	56.1	34	90
Lower Shell Plate R-1108-2	Position 1.1 Position 2.1	37 16.2	1.10	20	40.7 17.82	34 17	95 55
Lower Shell Plate R-1108-3	Position 1.1	51	1.10	0	56.1	34	90
All Beltline Region Welds (*Heat # 88112*)	Position 1.1 Position 2.1	46 11.5	1.10	-70	50.6 12.65	50.6 12.65	31 -45

NOTES:

(a) Chemistry Factors taken from Table 2-5.

(b) Initial RT$_{NDT}$ values are measured values; see Table 2-1.

(c) ΔRT$_{NDT}$ = CF * FF

(d) Margin = $2*(\sigma_i^2 + \sigma_A^2)^{1/2}$. Note all Surveillance Data is Credible.

(e) ART = IRT$_{NDT}$ + ΔRT$_{NDT}$ + M (This value was rounded per ASTM E29, using the "Rounding Method".)

TABLE 5-5
Calculation of the Comanche Peak Unit 1 ART Values for the 3/4T Location @ 36 EFPY

Material	Reg. Guide 1.99 Rev. 2 Method	CF[a] (°F)	¾ T FF	IRT$_{NDT}$[b] (°F)	ΔRT$_{NDT}$[c] (°F)	M[d] (°F)	ART[e] (°F)
Intermediate Shell Plate R-1107-1	Position 1.1	44	0.82	10	36.08	34	80
Intermediate Shell Plate R-1107-2	Position 1.1	44	0.82	-10	36.08	34	60
Intermediate Shell Plate R-1107-3	Position 1.1	37	0.82	10	30.34	30.34	71
Lower Shell Plate R-1108-1	Position 1.1	51	0.82	0	41.82	34	76
Lower Shell Plate R-1108-2	Position 1.1 / Position 2.1	37 / 16.2	0.82	20	30.34 / 13.28	30.34 / 13.28	81 / 47
Lower Shell Plate R-1108-3	Position 1.1	51	0.82	0	41.82	34	76
All Beltline Region Welds (*Heat # 88112*)	Position 1.1 / Position 2.1	46 / 11.5	0.82	-70	37.72 / 9.43	37.72 / 9.43	5 / -51

NOTES:

(a) Chemistry Factors taken from Table 2-5.

(b) Initial RT$_{NDT}$ values are measured values; see Table 2-1.

(c) ΔRT$_{NDT}$ = CF * FF

(d) Margin = $2*(\sigma_i^2 + \sigma_A^2)^{1/2}$. Note all Surveillance Data is Credible.

(e) ART = IRT$_{NDT}$ + ΔRT$_{NDT}$ + M (This value was rounded per ASTM E29, using the "Rounding Method".)

TABLE 5-6

Calculation of the Comanche Peak Unit 2 ART Values for the 1/4T Location @ 36 EFPY

Material	Reg. Guide 1.99 Rev. 2 Method	$CF^{(a)}$ (°F)	¼ T FF	$IRT_{NDT}^{(b)}$ (°F)	$\Delta RT_{NDT}^{(c)}$ (°F)	$M^{(d)}$ (°F)	$ART^{(e)}$ (°F)
Intermediate Shell Plate R3807-1	Position 1.1	37	1.09	-20	40.33	34	54
Intermediate Shell Plate R3807-2	Position 1.1 Position 2.1	37 21.6	1.09	10	40.33 23.54	34 $34^{(f)}$	84 68
Intermediate Shell Plate R3807-3	Position 1.1	31	1.09	-20	33.79	33.79	48
Lower Shell Plate R3816-1	Position 1.1	31	1.09	-30	33.79	33.79	38
Lower Shell Plate R3816-2	Position 1.1	20	1.09	0	21.8	21.8	44
Lower Shell Plate R3816-3	Position 1.1	26	1.09	-40	28.34	28.34	17
Intermediate & Lower Shell Longitudinal Welds (*Heat # 89833*)	Position 1.1 Position 2.1	31.5 32.8	1.09	-50	34.34 35.75	34.34 $28.0^{(f)}$	19 14
Intermediate to Lower Shell Girth Weld (*Heat # 89833*)	Position 1.1 Position 2.1	31.5 32.8	1.09	-60	34.34 35.75	34.34 $28.0^{(f)}$	9 4

NOTES:

(a) Chemistry Factors taken from Table 2-5.

(b) Initial RT_{NDT} values are measured values; see Table 2-1.

(c) $\Delta RT_{NDT} = CF * FF$

(d) Margin $= 2*(\sigma_i^2 + \sigma_\Delta^2)^{1/2}$.

(e) ART $= IRT_{NDT} + \Delta RT_{NDT} + M$ (This value was rounded per ASTM E29, using the "Rounding Method".)

(f) The surveillance plate (*Inter. Shell Plate R3807-1*) data is not credible, while the surveillance weld data is credible[9].

TABLE 5-7
Calculation of the Comanche Peak Unit 2 ART Values for the 3/4T Location @ 36 EFPY

Material	Reg. Guide 1.99 Rev. 2 Method	CF[a] (°F)	¾ T FF	IRT$_{NDT}$[b] (°F)	ΔRT$_{NDT}$[c] (°F)	M[d] (°F)	ART[e] (°F)
Intermediate Shell Plate R3807-1	Position 1.1	37	0.80	-20	29.6	29.6	39
Intermediate Shell Plate R3807-2	Position 1.1 Position 2.1	37 21.6	0.80	10	29.6 17.28	29.6 34[f]	69 61
Intermediate Shell Plate R3807-3	Position 1.1	31	0.80	-20	24.8	24.8	30
Lower Shell Plate R3816-1	Position 1.1	31	0.80	-30	24.8	24.8	20
Lower Shell Plate R3816-2	Position 1.1	20	0.80	0	16.0	16.0	32
Lower Shell Plate R3816-3	Position 1.1	26	0.80	-40	20.8	20.8	2
Intermediate & Lower Shell Longitudinal Welds (Heat # 89833)	Position 1.1 Position 2.1	31.5 32.8	0.80	-50	25.2 26.24	25.2 26.24[f]	0 2
Intermediate to Lower Shell Girth Weld (Heat # 89833)	Position 1.1 Position 2.1	31.5 32.8	0.80	-60	25.2 26.24	25.2 26.24[f]	-10 -8

NOTES:

(a) Chemistry Factors taken from Table 2-5.

(b) Initial RT$_{NDT}$ values are measured values; see Table 2-1.

(c) ΔRT$_{NDT}$ = CF * FF

(d) Margin = $2*(\sigma_i^2 + \sigma_\Delta^2)^{1/2}$.

(e) ART = IRT$_{NDT}$ + ΔRT$_{NDT}$ + M (This value was rounded per ASTM E29, using the "Rounding Method".)

(f) The surveillance plate (Inter. Shell Plate R3807-1) data is not credible, while the surveillance weld data is credible[9].

Based on review of the ART values for both units, the Intermediate Shell Plate R-1107-1 from Comanche Peak Unit 1 is the most limiting material because it has the highest ART value. Contained in Table 5-8 is a summary of the limiting ARTs from both units. The values from Unit 1 are to be used in generation of the Comanche Peak Units 1 and 2 reactor vessel PT limit curves. These limiting curves will be presented in Section 6.

TABLE 5-8

Summary of the Limiting ART Values Used in the

Generation of the Comanche Peak Units 1 and 2 Heatup/Cooldown Curves

EFPY	¼ T Limiting ART	¾ T Limiting ART
Comanche Peak Unit 1		
36*	92	80
Comanche Peak Unit 2		
36	84	69

*   Used in the generation of the Comanche Peak Units 1 and 2 PT Limit Curves as
        presented in Section 6.

For simplicity, TXU has been operating with common of PT limit curves for both Units since initial startup and TXU would prefer to continue using common curves. The reasoning behind this is two-fold. 1) From temperatures equal to 60°F to 160°F, the allowable pressure will be limited by the "flange-notch" pressure of 621 psig (from 10CFR50 Appendix G). Thus, generating PT limits with a Unit 1 specific and Unit 2 specific ART value would still result in the same PT limit curve. 2) From temperatures beyond 160°F, the advantages of using common of PT limit curves clearly outweighs the negligible increase in the allowable pressure that is mathematically available for the Unit 2 vessel.

As a note, by comparing the approximate allowable pressure of the current PT limits (i.e., use K_{Ia} @ 16 EFPY) for 100°F/hr heatup to the allowable pressure generated herein (@ 36 EFPY) for the same heatup rate, there is already an approximate 450 to 500 psig increase in allowable pressure that is achieve from using the newer, less restrictive, ASME Code methodology (i.e., use of K_{Ic} at 36 EFPY). Thus, there is little added benefit in generating PT limits using ART values that are only 8 and 11°F apart.

6   HEATUP AND COOLDOWN PRESSURE-TEMPERATURE LIMIT CURVES

Pressure-temperature limit curves for normal heatup and cooldown of the primary reactor coolant system have been calculated for the pressure and temperature in the reactor vessel beltline region using the methods discussed in Sections 4 and 5 of this report. This approved methodology is also presented in WCAP-14040-NP-A, Revision 4.

Figures 6-1 and 6-3 present the limiting heatup curves without margins for possible instrumentation errors using heatup rates of 20, 60 and 100°F/hr applicable for the first 36 EFPY with and without the "Flange-Notch" requirement. These curves were generated using the1998 ASME Code Section XI, Appendix G. Figures 6-2 and 6-4 present the limiting cooldown curves without margins for possible instrumentation errors using cooldown rates of 0, 20, 40, 60 and 100°F/hr applicable for 36 EFPY with and without the "Flange-Notch" requirement. Again, these curves were generated using the1998 ASME Code Section XI, Appendix G. Allowable combinations of temperature and pressure for specific temperature change rates are below and to the right of the limit line shown in Figures 6-1 through 6-4. This is in addition to other criteria, which must be met before the reactor is made critical, as discussed below in the following paragraphs.

The reactor must not be made critical until pressure-temperature combinations are to the right of the criticality limit line shown in Figures 6-1 and 6-3. The straight-line portion of the criticality limit is at the minimum permissible temperature for the 2485 psig inservice hydrostatic test as required by Appendix G to 10 CFR Part 50. The governing equation for the hydrostatic test is defined in the1998 ASME Code Section XI, Appendix G as follows:

$$1.5 \, K_{Im} < K_{Ic}$$

where,

> K_{Im} is the stress intensity factor covered by membrane (pressure) stress,
>
> $K_{Ic} = 33.2 + 20.734 \, e^{[0.02 \, (T - RT_{NDT})]}$,
>
> .   T is the minimum permissible metal temperature, and
>
> RT_{NDT} is the metal reference nil-ductility temperature.

The criticality limit curve specifies pressure-temperature limits for core operation to provide additional margin during actual power production as specified in Reference 3. The pressure-temperature limits for core operation (except for low power physics tests) are that the reactor vessel must be at a temperature equal to or higher than the minimum temperature required for the inservice hydrostatic test, and at least 40°F higher than the minimum permissible temperature in the corresponding pressure-temperature curve for heatup and cooldown calculated as described in Section 5 of this report. For the heatup and cooldown curves without margins for instrumentation errors, the minimum temperatures for the in service hydrostatic leak tests for the Comanche Peak Units 1 and 2 reactor vessel at 36 EFPY is 152°F. The vertical line drawn from these points on the pressure-temperature curve, intersecting a curve 40°F higher than the pressure-temperature limit curve constitutes the limit for core operation for the reactor vessel.

Figures 6-1 through 6-4 define all of the above limits for ensuring prevention of non-ductile failure for the Comanche Peak Units 1 and 2 reactor vessel for 36 EFPY with and without the "Flange-Notch" requirement[3]. The data points used for the heatup and cooldown pressure-temperature limit curves shown in Figures 6-1 through 6-4 are presented in Tables 6-1 through 6-4.

MATERIAL PROPERTY BASIS

LIMITING MATERIAL: Intermediate Shell Plate R-1107-1 (*from Comanche Peak Unit 1*)

LIMITING ART VALUES AT 36 EFPY: 1/4T,   92°F

                                          3/4T,   80°F
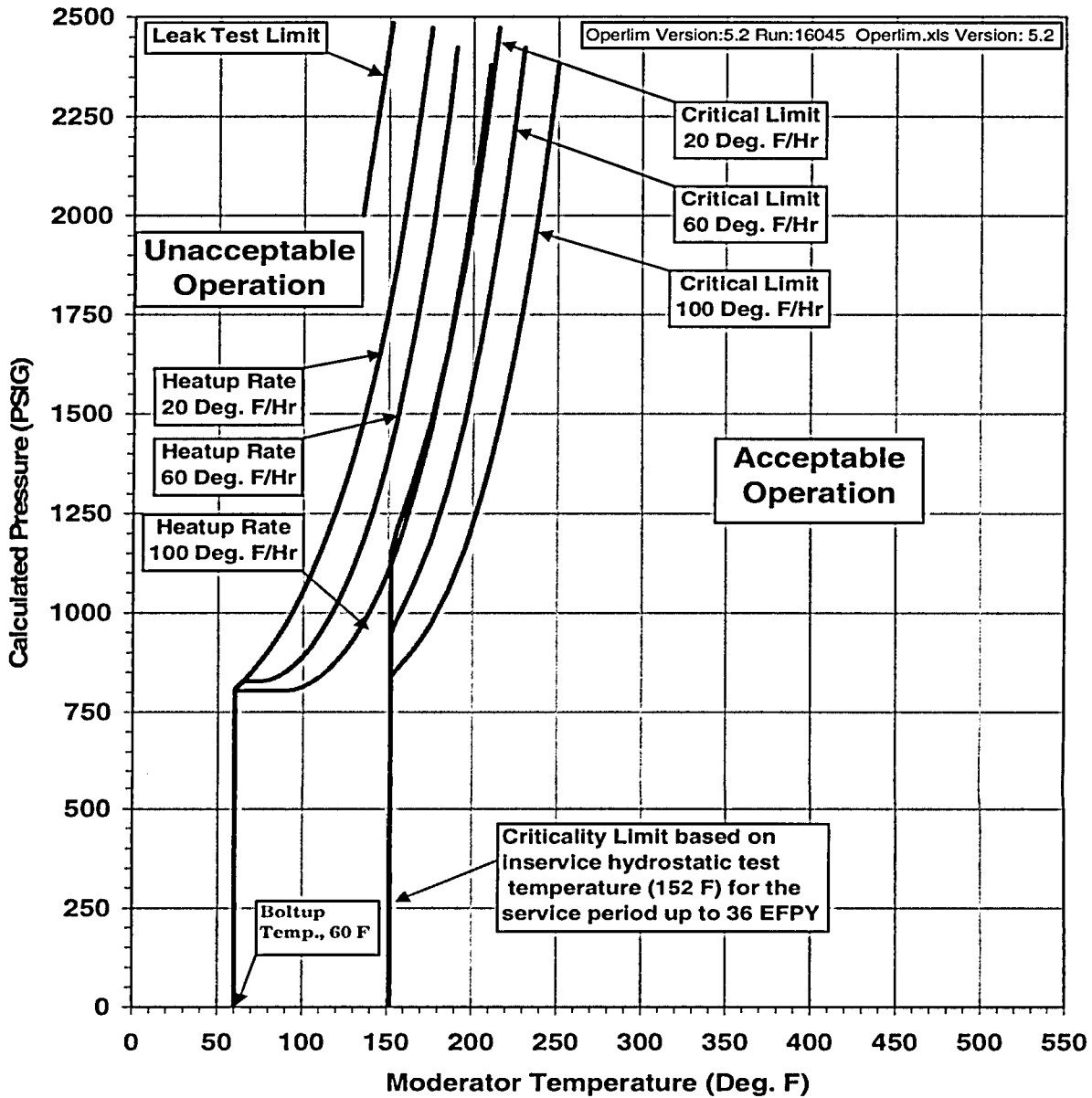
Figure 6-1   **Comanche Peak Units 1 and 2 Reactor Coolant System Heatup Limitations (Heatup Rates of 20, 60 and 100°F/hr) Applicable for the First 36 EFPY (w/o the "Flange-Notch" & Margins for Instrumentation Errors) Using 1998 App. G Methodology (w/K$_{Ic}$)**

MATERIAL PROPERTY BASIS

LIMITING MATERIAL: Intermediate Shell Plate R-1107-1 *(from Comanche Peak Unit 1)*

LIMITING ART VALUES AT 36 EFPY: 1/4T,   92°F

                                          3/4T,   80°F
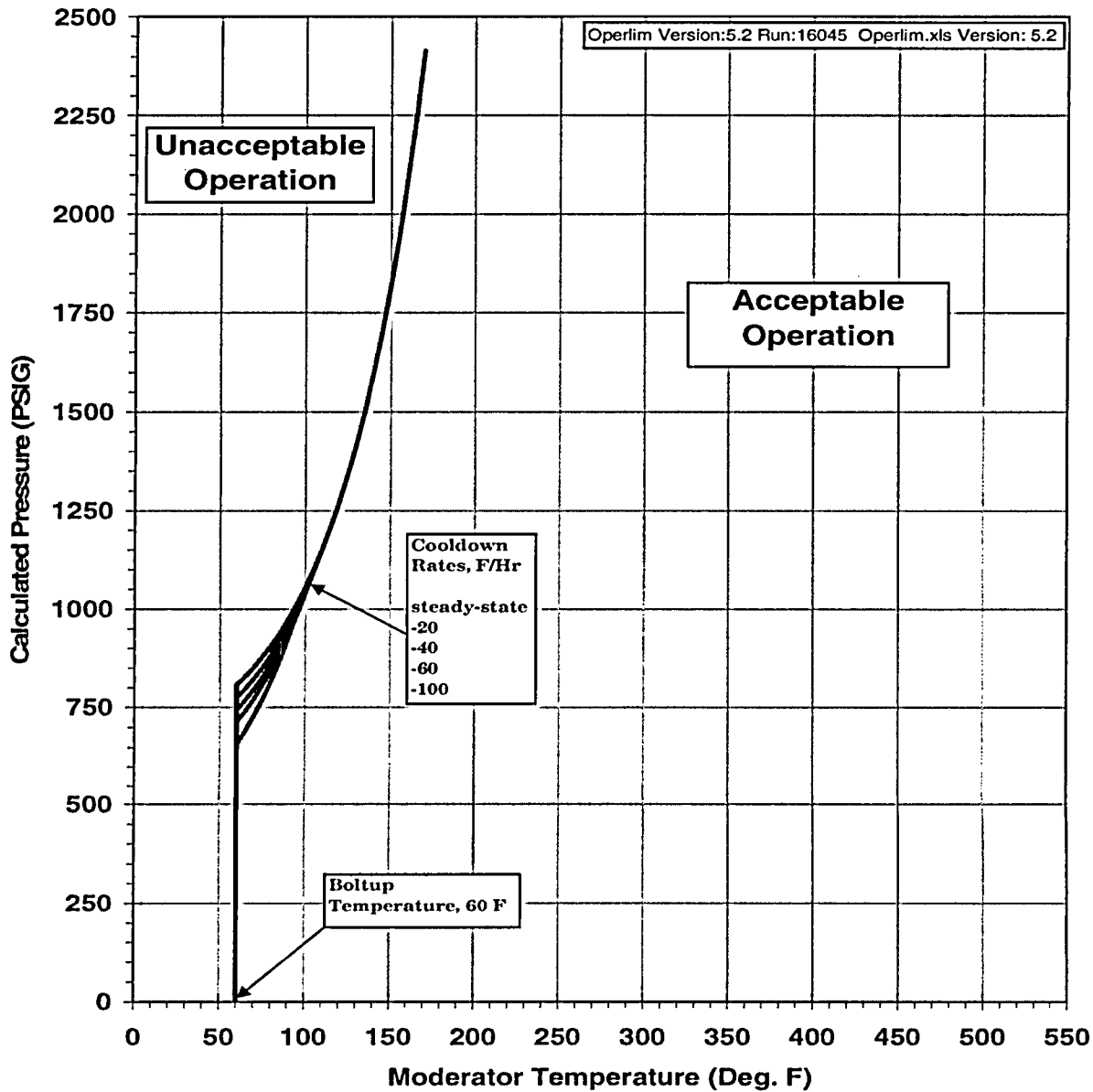
Figure 6-2   **Comanche Peak Units 1 and 2 Reactor Coolant System Cooldown Limitations (Cooldown Rates up to 100°F/hr) Applicable for the First 36 EFPY (w/o the "Flange-Notch" & Margins for Instrumentation Errors) Using 1998 App. G Methodology (w/K_{Ic})**

MATERIAL PROPERTY BASIS

LIMITING MATERIAL: Intermediate Shell Plate R-1107-1 (*from Comanche Peak Unit 1*)
LIMITING ART VALUES AT 36 EFPY: 1/4T,   92°F
                                             3/4T,   80°F
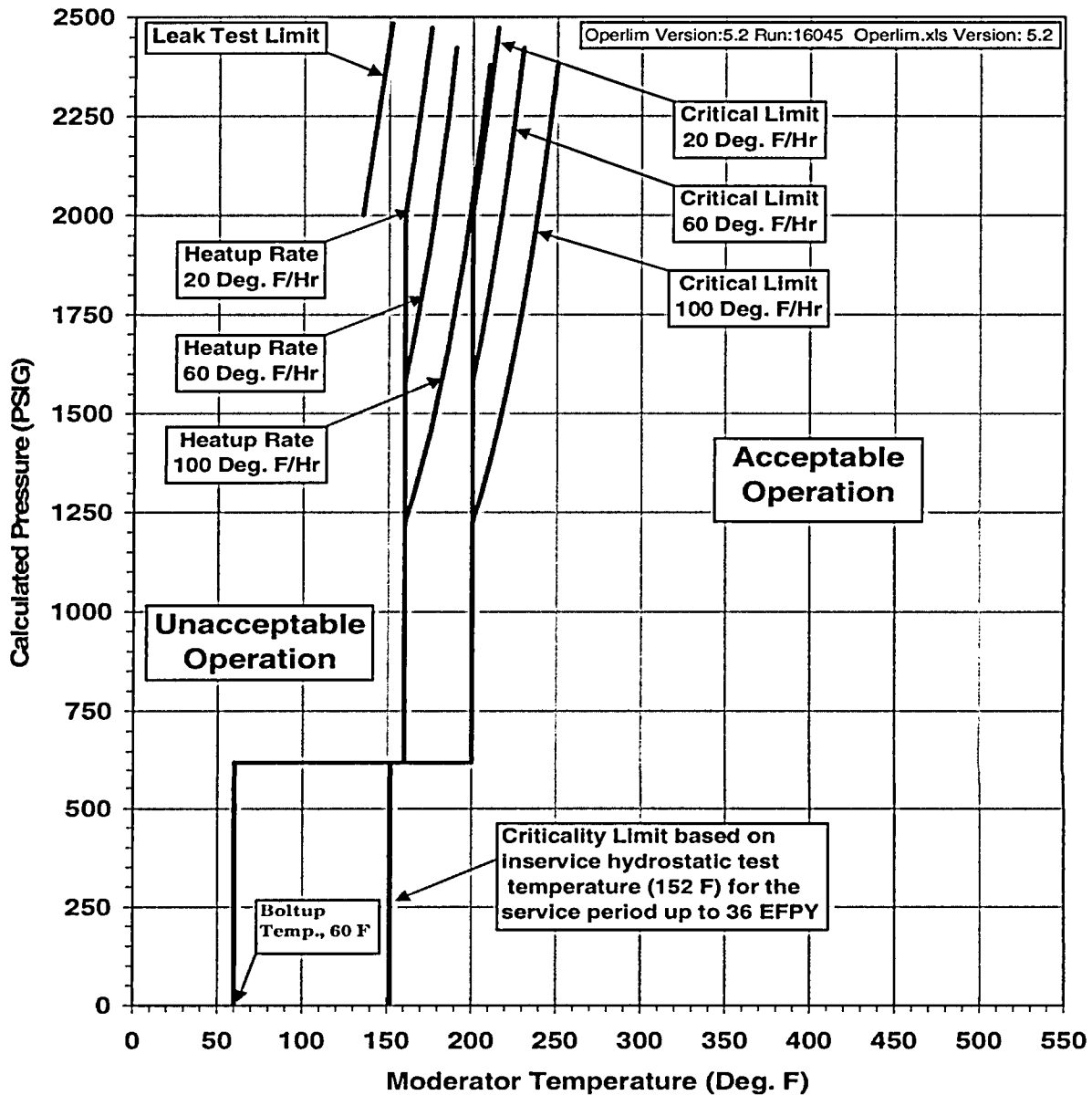
Figure 6-3   Comanche Peak Units 1 and 2 Reactor Coolant System Heatup Limitations (Heatup
              Rates of 20, 60 and 100°F/hr) Applicable for the First 36 EFPY (w/ the "Flange-Notch"
              but w/o Margins for Instrumentation Errors) Using 1998 App. G Methodology (w/K$_{Ic}$)

MATERIAL PROPERTY BASIS

LIMITING MATERIAL: Intermediate Shell Plate R-1107-1 (*from Comanche Peak Unit 1*)
LIMITING ART VALUES AT 36 EFPY: 1/4T,   92°F
                                             3/4T,   80°F
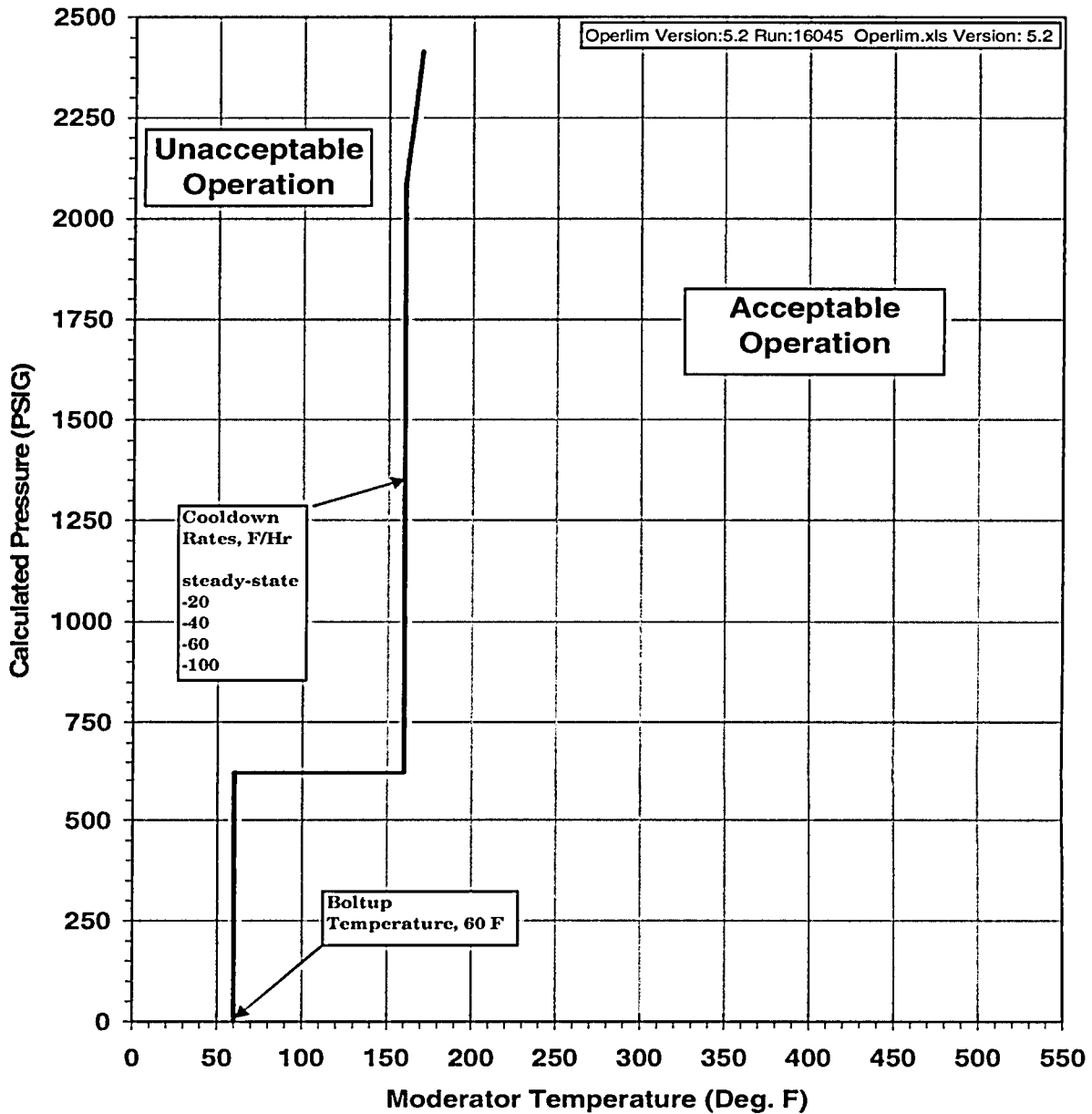
Figure 6-4   Comanche Peak Units 1 and 2 Reactor Coolant System Cooldown Limitations
              (Cooldown Rates up to 100°F/hr) Applicable for the First 36 EFPY (w/ the "Flange-
              Notch" but w/o Margins for Instrumentation Errors) Using 1998 App. G Methodology
              (w/K_{Ic})

TABLE 6-1

36 EFPY Heatup Curve Data Points Using 1998 App. G Methodology

(w/K_{IC}, w/o Flange Notch & Uncertainties for Instrumentation Errors)

20 Heatup		Critical. Limit		60 Heatup		Critical. Limit		100 Heatup		Critical. Limit	
T (°F)	P (psig)	T (°F)	P (psig)	T (°F)	P (psig)	T (°F)	P (psig)	T (°F)	P (psig)	T (°F)	P (psig)
60	0	152	0	60	0	152	0	60	0	152	0
60	808	152	808	60	808	152	828	60	803	152	803
65	829	152	852	65	828	152	831	65	803	152	803
70	852	152	878	70	828	152	832	70	803	152	806
75	878	152	906	75	828	152	838	75	803	152	807
80	906	152	938	80	831	152	841	80	803	152	814
85	938	152	972	85	838	152	851	85	803	152	815
90	972	152	1011	90	851	152	868	90	803	152	824
95	1011	152	1053	95	868	152	890	95	806	152	827
100	1053	152	1100	100	890	152	916	100	814	152	839
105	1100	152	1152	105	916	152	947	105	824	155	857
110	1152	155	1208	110	947	155	982	110	839	160	879
115	1208	160	1266	115	982	160	1023	115	857	165	905
120	1266	165	1329	120	1023	165	1069	120	879	170	935
125	1329	170	1399	125	1069	170	1120	125	905	175	970
130	1399	175	1477	130	1120	175	1178	130	935	180	1009
135	1477	180	1562	135	1178	180	1242	135	970	185	1054
140	1562	185	1657	140	1242	185	1314	140	1009	190	1104
145	1657	190	1761	145	1314	190	1393	145	1054	195	1160
150	1761	195	1877	150	1393	195	1481	150	1104	200	1223
155	1877	200	2004	155	1481	200	1579	155	1160	205	1293
160	2004	205	2145	160	1579	205	1687	160	1223	210	1370
165	2145	210	2300	165	1687	210	1806	165	1293	215	1457
170	2300	215	2472	170	1806	215	1938	170	1370	220	1552
175	2472			175	1938	220	2084	175	1457	225	1658
				180	2084	225	2245	180	1552	230	1775
				185	2245	230	2423	185	1658	235	1904
				190	2423			190	1775	240	2047
								195	1904	245	2205
								200	2047	250	2379
								205	2205	250	2459
								210	2379		

Leak Test Limit	Temp. (°F)	135	2000								
	Pressure (psig)	152	2485								

TABLE 6-2
36 EFPY Cooldown Curve Data Points Using 1998 App. G Methodology
(w/K_{IC}, w/o Flange Notch & Uncertainties for Instrumentation Errors)

Steady State		20°F/hr.		40°F/hr.		60°F/hr.		100°F/hr.	
T (°F)	P (psig)	T (°F)	P (psig)	T (°F)	P (psig)	T (°F)	P (psig)	T (°F)	P (psig)
60	0	60	0	60	0	60	0	60	0
60	808	60	775	60	744	60	713	60	658
65	829	65	798	65	769	65	741	65	691
70	852	70	824	70	797	70	771	70	729
75	878	75	852	75	827	75	805	75	770
80	906	80	883	80	862	80	843	80	817
85	938	85	917	85	899	85	885	85	868
90	972	90	955	90	941	90	931	90	925
95	1011	95	997	95	988	95	982	95	982
100	1053	100	1044	100	1039	100	1039	100	1039
105	1100	105	1095	105	1095	105	1095	105	1095
110	1152	110	1152	110	1152	110	1152	110	1152
115	1209	115	1209	115	1209	115	1209	115	1209
120	1272	120	1272	120	1272	120	1272	120	1272
125	1342	125	1342	125	1342	125	1342	125	1342
130	1419	130	1419	130	1419	130	1419	130	1419
135	1504	135	1504	135	1504	135	1504	135	1504
140	1599	140	1599	140	1599	140	1599	140	1599
145	1703	145	1703	145	1703	145	1703	145	1703
150	1818	150	1818	150	1818	150	1818	150	1818
155	1946	155	1946	155	1946	155	1946	155	1946
160	2086	160	2086	160	2086	160	2086	160	2086
165	2242	165	2242	165	2242	165	2242	165	2242
170	2414	170	2414	170	2414	170	2414	170	2414

TABLE 6-3
36 EFPY Heatup Curve Data Points Using 1998 App. G Methodology
(w/K_{IC} & Flange Notch, w/o Uncertainties for Instrumentation Errors)

20 Heatup		Critical. Limit		60 Heatup		Critical. Limit		100 Heatup		Critical. Limit	
T (°F)	P (psig)	T (°F)	P (psig)	T (°F)	P (psig)	T (°F)	P (psig)	T (°F)	P (psig)	T (°F)	P (psig)
60	0	151	0	60	0	151	0	60	0	151	0
60	621	151	621	60	621	151	621	60	621	151	621
65	621	151	621	65	621	151	621	65	621	151	621
70	621	151	621	70	621	151	621	70	621	151	621
75	621	151	621	75	621	151	621	75	621	151	621
80	621	151	621	80	621	151	621	80	621	151	621
85	621	151	621	85	621	151	621	85	621	151	621
90	621	151	621	90	621	151	621	90	621	151	621
95	621	151	621	95	621	151	621	95	621	151	621
100	621	151	621	100	621	151	621	100	621	151	621
105	621	151	621	105	621	151	621	105	621	151	621
110	621	155	621	110	621	155	621	110	621	155	621
115	621	160	621	115	621	160	621	115	621	160	621
120	621	165	621	120	621	165	621	120	621	165	621
125	621	170	621	125	621	170	621	125	621	170	621
130	621	175	621	130	621	175	621	130	621	175	621
135	621	180	621	135	621	180	621	135	621	180	621
140	621	185	621	140	621	185	621	140	621	185	621
145	621	190	621	145	621	190	621	145	621	190	621
150	621	195	621	150	621	195	621	150	621	195	621
155	621	200	621	155	621	200	621	155	621	200	1223
160	621	200	2004	160	621	200	1579	160	621	205	1293
160	2004	205	2145	160	1579	205	1687	160	1223	210	1370
165	2145	210	2300	165	1687	210	1806	165	1293	215	1457
170	2300	215	2472	170	1806	215	1938	170	1370	220	1552
175	2472			175	1938	220	2084	175	1457	225	1658
				180	2084	225	2245	180	1552	230	1775
				185	2245	230	2423	185	1658	235	1904
				190	2423			190	1775	240	2047
								195	1904	245	2205
								200	2047	250	2379
								205	2205		
								210	2379		
Leak Test Limit		Temp. (°F)		135	2000						
		Pressure (psig)		152	2485						

TABLE 6-4

36 EFPY Cooldown Curve Data Points Using 1998 App. G Methodology

(w/K$_{IC}$ & Flange Notch, w/o Uncertainties for Instrumentation Errors)

Steady State		20°F/hr.		40°F/hr.		60°F/hr.		100°F/hr.	
T (°F)	P (psig)	T (°F)	P (psig)	T (°F)	P (psig)	T (°F)	P (psig)	T (°F)	P (psig)
60	0	60	0	60	0	60	0	60	0
60	621	60	621	60	621	60	621	60	621
65	621	65	621	65	621	65	621	65	621
70	621	70	621	70	621	70	621	70	621
75	621	75	621	75	621	75	621	75	621
80	621	80	621	80	621	80	621	80	621
85	621	85	621	85	621	85	621	85	621
90	621	90	621	90	621	90	621	90	621
95	621	95	621	95	621	95	621	95	621
100	621	100	621	100	621	100	621	100	621
105	621	105	621	105	621	105	621	105	621
110	621	110	621	110	621	110	621	110	621
115	621	115	621	115	621	115	621	115	621
120	621	120	621	120	621	120	621	120	621
125	621	125	621	125	621	125	621	125	621
130	621	130	621	130	621	130	621	130	621
135	621	135	621	135	621	135	621	135	621
140	621	140	621	140	621	140	621	140	621
145	621	145	621	145	621	145	621	145	621
150	621	150	621	150	621	150	621	150	621
155	621	155	621	155	621	155	621	155	621
160	621	160	621	160	621	160	621	160	621
160	2086	160	2086	160	2086	160	2086	160	2086
165	2242	165	2242	165	2242	165	2242	165	2242
170	2414	170	2414	170	2414	170	2414	170	2414

7 REFERENCES

1. Regulatory Guide 1.99, Revision 2, "Radiation Embrittlement of Reactor Vessel Materials," U.S. Nuclear Regulatory Commission, May 1988.

2. WCAP-14040-NP-A, Revision 4, "Methodology used to Develop Cold Overpressure Mitigating System Setpoints and RCS Heatup and Cooldown Limit Curves", J.D. Andrachek, et. al., May 2004.

3. Code of Federal Regulations, 10 CFR Part 50, Appendix G, "Fracture Toughness Requirements," U.S. Nuclear Regulatory Commission, Washington, D.C., Federal Register, Volume 60, No. 243, dated December 19, 1995.

4. "Fracture Toughness Requirements", Branch Technical Position MTEB 5-2, Chapter 5.3.2 in Standard Review Plan for the Review of Safety Analysis Reports for Nuclear Power Plants, LWR Edition, NUREG-0800, 1981.

5. Combustion Engineering Certified Material Test Reports for Comanche Peak Unit 1 Reactor Vessel Intermediate and Lower Shell Plates:
   - Intermediate Shell Plate R-1107-1: Combustion Engineering, Inc., Metallurgical Research and Development Dept., Contract No. 10773, Job No. 732124-001, 11-27-74.
   - Intermediate Shell Plate R-1107-2: Combustion Engineering, Inc., Metallurgical Research and Development Dept., Contract No. 10773, Job No. 732124-003, 11/27/74.
   - Intermediate Shell Plate R-1107-3: Combustion Engineering, Inc., Metallurgical Research and Development Dept., Contract No. 10773, Job No. 732124-005, 11/20/74.
   - Lower Shell Plate R-1108-1: Combustion Engineering, Inc., Metallurgical Research and Development Dept., Contract No. 10773, Job No. 732142-001, 9-8-1975.
   - Lower Shell Plate R-1108-2: Combustion Engineering, Inc., Metallurgical Research and Development Dept., Contract No. 10773, Job No. 732142-003, 9-5-1975.
   - Lower Shell Plate R-1108-3: Combustion Engineering, Inc., Metallurgical Research and Development Dept., Contract No. 10773, Job No. 732142-005, 9-8-1975.

6. TU Electric # TXX-94172, "Comanche Peak Steam Electric Station (CPSES) Docket Nos. 50-445 and 50-446 Generic Letter (GL) 92-01, Revision 1, 'Reactor Vessel Structural Integrity,' Texas Utilities Electric Company, Comanche Peak Steam Electric Station, Unit Nos. 1 and 2 (TAC Nos. M83451 and M83452)," William J. Cahill Jr., Dated June 20, 1994 (*Plus Enclosures*).

7. TU Electric # CPSES-9706134, "Comanche Peak Steam Electric Station (CPSES) Docket Nos. 50-445 and 50-446 Response to NRC Request for Additional Information Regarding NRC Generic Letter 92-01, Revision 1, Supplement 1," C. Lance Terry, Dated December 31, 1997 (*Plus Enclosures*).

8. CE Report NPSD-1039, Rev. 2, "Best Estimate Copper and Nickel Values in CE Fabricated Reactor Vessel Welds", CEOG Task 902, By the CE Owners Group, June 1997.

9. Regulatory Guide 1.190, "Calculational and Dosimetry Methods for Determining Pressure Vessel Neutron Fluence," March 2001.

10.   WCAP-16277-NP, "Analysis of Capsule X from the TXU Energy Comanche Peak Unit 2 Reactor Vessel Radiation Surveillance Program," T.J. Laubham, et. al., September 2004.

11.   WCAP-15144, "Analysis of Capsule Y from the TU Electric Company Comanche Peak Unit 1 Reactor Vessel Radiation Surveillance Program," T.J. Laubham, et. al., January 1999.

12.   Section XI of the ASME Boiler and Pressure Vessel Code, Appendix G, "Fracture Toughness Criteria for Protection Against Failure." Dated December 1998, through 2000 Addendum.

13.   1989 Section III, Division 1 of the ASME Boiler and Pressure Vessel Code, Paragraph NB-2331, "Material for Vessels"

14.   WCAP-9806, Revision 3, "The Nuclear Design and Core Physics Characteristics of the Comanche Peak Unit 1 Nuclear Power Plant Cycle 1," April 1990.

15.   WCAP-13094, "The Nuclear Design and Core Physics Characteristics of the Comanche Peak Unit 1 Nuclear Power Plant Cycle 2," December 1991.

16.   WCAP-13613, "The Nuclear Design and Core Physics Characteristics of the Comanche Peak Unit 1 Nuclear Power Plant Cycle 3," January 1993.

17.   CPSES-9804980, "Reactor Core Data to Support the Westinghouse Evaluation of the CPSES Unit 1 Reactor Vessel Material Surveillance Specimen (Capsule "Y")," September 1998.

18.   CPSES-200401980, "Transmittal of Design Information for Unit 1 Fluence Analysis," August 2004.

19.   RSICC Computer Code Collection CCC-650, "DOORS 3.1, One, Two- and Three-Dimensional Discrete Ordinates Neutron/Photon Transport Code System," August 1996.

20.   RSIC Data Library Collection DLC-185, "BUGLE-96, Coupled 47 Neutron, 20 Gamma-Ray Group Cross Section Library Derived from ENDF/B-VI for LWR Shielding and Pressure Vessel Dosimetry Applications," March 1996.

APPENDIX A

VALIDATION OF THE RADIATION TRANSPORT MODELS

BASED ON NEUTRON DOSIMETRY MEASUREMENTS

A.1 NEUTRON DOSIMETRY

Comparisons of measured dosimetry results to both the calculated and least squares adjusted values for all surveillance capsules withdrawn from service to date at Comanche Peak Unit 1 are described herein. The sensor sets from these capsules have been analyzed in accordance with the current dosimetry evaluation methodology described in Regulatory Guide 1.190, "Calculational and Dosimetry Methods for Determining Pressure Vessel Neutron Fluence."[A-1] One of the main purposes for presenting this material is to demonstrate that the overall measurements agree with the calculated and least squares adjusted values to within ± 20% as specified by Regulatory Guide 1.190, thus serving to validate the calculated neutron exposures previously reported in Section 3.2 of this report. This information may also be useful in the future, in particular, as least squares adjustment techniques become accepted in the regulatory environment.

A.1.1 Sensor Reaction Rate Determinations

In this section, the results of the evaluations of the two neutron sensor sets withdrawn to date as part of the Comanche Peak Unit 1 Reactor Vessel Materials Surveillance Program are presented. The capsule designation, location within the reactor, and time of withdrawal of each of these dosimetry sets were as follows:

Capsule ID	Azimuthal Location	Withdrawal Time	Irradiation Time [EFPY]
U	31.5° Dual	End of Cycle 1	0.91
Y	29° Dual	End of Cycle 6	6.24

The azimuthal locations included in the above tabulation represent the first octant equivalent azimuthal angle of the geometric center of the respective surveillance capsules.

The passive neutron sensors included in the evaluations of Surveillance Capsules U and Y are summarized as follows:

Sensor Material	Reaction Of Interest	Capsule U	Capsule Y
Copper	$^{63}Cu(n,\alpha)^{60}Co$	X	X
Iron	$^{54}Fe(n,p)^{54}Mn$	X	X
Nickel	$^{58}Ni(n,p)^{58}Co$	X	X
Uranium-238	$^{238}U(n,f)^{137}Cs$	X	X
Neptunium-237	$^{237}Np(n,f)^{137}Cs$	X	X
Cobalt-Aluminum*	$^{59}Co(n,\gamma)^{60}Co$	X	X

* The cobalt-aluminum measurements for this plant include both bare wire and cadmium-covered sensors.

Since all of the dosimetry monitors were accommodated within the dosimeter block centered at the radial, azimuthal, and axial center of the material test specimen array, gradient corrections were not required for these reaction rates. Pertinent physical and nuclear characteristics of the passive neutron sensors are listed in Table A-1.

The use of passive monitors such as those listed above does not yield a direct measure of the energy dependent neutron flux at the point of interest. Rather, the activation or fission process is a measure of the integrated effect that the time and energy dependent neutron flux has on the target material over the course of the irradiation period. An accurate assessment of the average neutron flux level incident on the various monitors may be derived from the activation measurements only if the irradiation parameters are well known. In particular, the following variables are of interest:

- the measured specific activity of each monitor,

- the physical characteristics of each monitor,

- the operating history of the reactor,

- the energy response of each monitor, and

- the neutron energy spectrum at the monitor location.

Results from the radiometric counting of the neutron sensors from Capsules U and Y are documented in References A-2 and A-3. In all cases, the radiometric counting followed established ASTM procedures. Following sample preparation and weighing, the specific activity of each sensor was determined by means of a high-resolution gamma spectrometer. For the copper, iron, nickel, and cobalt-aluminum sensors, these analyses were performed by direct counting of each of the individual samples. In the case of the uranium and neptunium fission sensors, the analyses were carried out by direct counting preceded by dissolution and chemical separation of cesium from the sensor material.

The irradiation history of the reactor over the irradiation periods experienced by Capsules U (April 1990 – October 1991) and Y (April 1990 – March 1998) was based on the monthly power generation of Comanche Peak Unit 1 from initial reactor criticality through the end of the dosimetry evaluation period. For the sensor sets utilized in the surveillance capsules, the half-lives of the product isotopes are long enough that a monthly histogram describing reactor operation has proven to be an adequate representation for use in radioactive decay corrections for the reactions of interest in the exposure evaluations. The irradiation history applicable to Comanche Peak Unit 1 through the end of Cycle 10 (April 1990 – March 2004) is given in Table A-2.

Having the measured specific activities, the physical characteristics of the sensors, and the operating history of the reactor, reaction rates referenced to full-power operation were determined from the following equation:

$$R = \frac{A}{N_0\, F\, Y\, \sum \dfrac{P_j}{P_{ref}}\, C_j [1 - e^{-\lambda t_j}][e^{-\lambda t_d}]}$$

where:

R   =   Reaction rate averaged over the irradiation period and referenced to operation at a core power level of P_{ref} (rps/nucleus).

A   =   Measured specific activity (dps/gm).

N_0 =   Number of target element atoms per gram of sensor.

F   =   Atom fraction of the target isotope in the target element.

Y   =   Number of product atoms produced per reaction.

P_j =   Average core power level during irradiation period j (MW).

P_{ref} =   Maximum or reference power level of the reactor (MW).

C_j =   Calculated ratio of φ(E > 1.0 MeV) during irradiation period j to the time weighted average φ(E > 1.0 MeV) over the entire irradiation period.

λ =   Decay constant of the product isotope (1/sec).

t_j =   Length of irradiation period j (sec).

t_d =   Decay time following irradiation period j (sec).

and the summation is carried out over the total number of monthly intervals comprising the irradiation period.

In the equation describing the reaction rate calculation, the ratio $[P_j]/[P_{ref}]$ accounts for month-by-month variation of reactor core power level within any given fuel cycle as well as over multiple fuel cycles. The ratio C_j, which was calculated for each fuel cycle using the transport methodology discussed in Section 3.2, accounts for the change in sensor reaction rates caused by variations in flux level induced by changes in core spatial power distributions from fuel cycle to fuel cycle. For a single-cycle irradiation, C_j is normally taken to be 1.0. However, for multiple-cycle irradiations, particularly those employing low leakage fuel management, the additional C_j term should be employed. The impact of changing flux levels for constant power operation can be quite significant for sensor sets that have been irradiated for many cycles in a reactor that has transitioned from non-low leakage to low leakage fuel management or for sensor sets contained in surveillance capsules that have been moved from one capsule location to another. The fuel cycle specific neutron flux values along with the computed values for C_j are listed in Table A-3. These flux values represent the cycle dependent results at the radial and azimuthal center of the respective capsules at the axial elevation of the active fuel midplane.

Prior to using the measured reaction rates in the least-squares evaluations of the dosimetry sensor sets, additional corrections were made to the [238]U measurements to account for the presence of [235]U impurities in the sensors as well as to adjust for the build-in of plutonium isotopes over the course of the irradiation. Corrections were also made to the [238]U and [237]Np sensor reaction rates to account for gamma ray induced fission reactions that occurred over the course of the capsule irradiations. The correction factors applied to the Comanche Peak Unit 1 fission sensor reaction rates are summarized as follows:

Correction	Capsule U	Capsule Y
^{235}U Impurity/Pu Build-in	0.872	0.826
^{238}U(γ,f)	0.966	0.967
Net ^{238}U Correction	0.842	0.799
^{237}Np(γ,f)	0.990	0.990

These factors were applied in a multiplicative fashion to the decay corrected uranium and neptunium fission sensor reaction rates.

Results of the sensor reaction rate determinations for Capsules U and Y are given in Table A-4. In Table A-4, the measured specific activities, decay corrected saturated specific activities, and computed reaction rates for each sensor indexed to the radial center of the capsule are listed. The fission sensor reaction rates are listed both with and without the applied corrections for ^{238}U impurities, plutonium build-in, and gamma ray induced fission effects.

A.1.2 Least Squares Evaluation of Sensor Sets

Least squares adjustment methods provide the capability of combining the measurement data with the corresponding neutron transport calculations resulting in a Best Estimate neutron energy spectrum with associated uncertainties. Best Estimates for key exposure parameters such as φ(E > 1.0 MeV) or dpa/s along with their uncertainties are then easily obtained from the adjusted spectrum. In general, the least squares methods, as applied to surveillance capsule dosimetry evaluations, act to reconcile the measured sensor reaction rate data, dosimetry reaction cross-sections, and the calculated neutron energy spectrum within their respective uncertainties. For example,

$$R_i \pm \delta_{R_i} = \sum_g (\sigma_{ig} \pm \delta_{\sigma_{ig}})(\varphi_g \pm \delta_{\varphi_g})$$

relates a set of measured reaction rates, R_i, to a single neutron spectrum, φ_g, through the multigroup dosimeter reaction cross-section, σ_{ig}, each with an uncertainty δ. The primary objective of the least squares evaluation is to produce unbiased estimates of the neutron exposure parameters at the location of the measurement.

For the least squares evaluation of the Comanche Peak Unit 1 surveillance capsule dosimetry, the FERRET code[A-4] was employed to combine the results of the plant specific neutron transport calculations and sensor set reaction rate measurements to determine best-estimate values of exposure parameters (φ(E > 1.0 MeV) and dpa) along with associated uncertainties for the two in-vessel capsules withdrawn to date.

The application of the least squares methodology requires the following input:

    1 - The calculated neutron energy spectrum and associated uncertainties at the measurement location.

    2 - The measured reaction rates and associated uncertainty for each sensor contained in the multiple foil set.

    3 - The energy dependent dosimetry reaction cross-sections and associated uncertainties for each sensor contained in the multiple foil sensor set.

For the Comanche Peak Unit 1 application, the calculated neutron spectrum was obtained from the results of plant specific neutron transport calculations described in Section 3.2 of this report. The sensor reaction rates were derived from the measured specific activities using the procedures described in Section A.1.1. The dosimetry reaction cross-sections and uncertainties were obtained from the SNLRML dosimetry cross-section library[A-5]. The SNLRML library is an evaluated dosimetry reaction cross-section compilation recommended for use in LWR evaluations by ASTM Standard E1018, "Application of ASTM Evaluated Cross-Section Data File, Matrix E 706 (IIB)".

The uncertainties associated with the measured reaction rates, dosimetry cross-sections, and calculated neutron spectrum were input to the least squares procedure in the form of variances and covariances. The assignment of the input uncertainties followed the guidance provided in ASTM Standard E 944, "Application of Neutron Spectrum Adjustment Methods in Reactor Surveillance."

The following provides a summary of the uncertainties associated with the least squares evaluation of the Comanche Peak Unit 1 surveillance capsule sensor sets.

Reaction Rate Uncertainties

The overall uncertainty associated with the measured reaction rates includes components due to the basic measurement process, irradiation history corrections, and corrections for competing reactions. A high level of accuracy in the reaction rate determinations is assured by utilizing laboratory procedures that conform to the ASTM National Consensus Standards for reaction rate determinations for each sensor type.
After combining all of these uncertainty components, the sensor reaction rates derived from the counting and data evaluation procedures were assigned the following net uncertainties for input to the least squares evaluation:

Reaction	Uncertainty
$^{63}Cu(n,\alpha)^{60}Co$	5%
$^{54}Fe(n,p)^{54}Mn$	5%
$^{58}Ni(n,p)^{58}Co$	5%
$^{238}U(n,f)^{137}Cs$	10%
$^{237}Np(n,f)^{137}Cs$	10%
$^{59}Co(n,\gamma)^{60}Co$	5%

These uncertainties are given at the 1σ level.
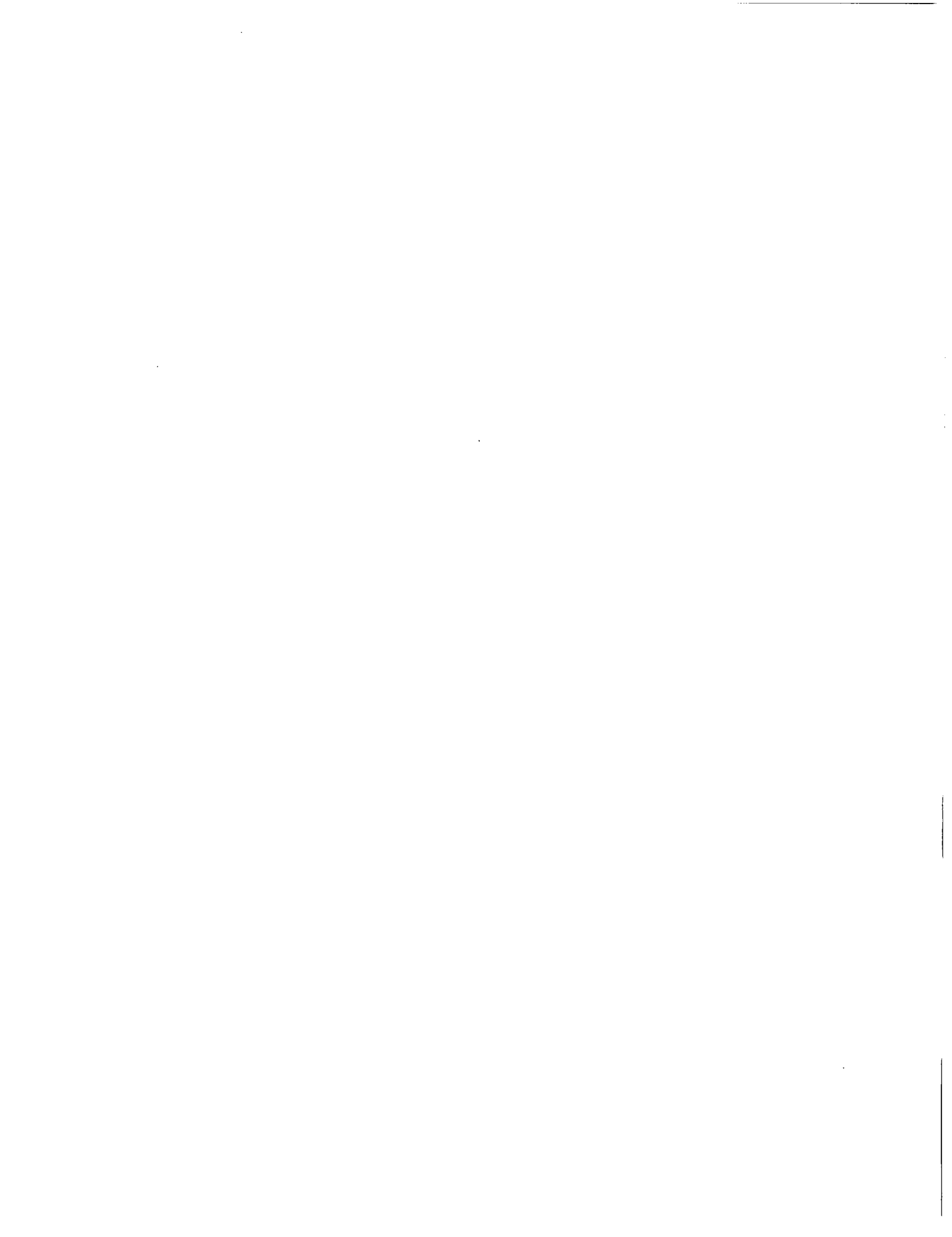
Dosimetry Cross-Section Uncertainties

The reaction rate cross-sections used in the least squares evaluations were taken from the SNLRML library. This data library provides reaction cross-sections and associated uncertainties, including covariances, for 66 dosimetry sensors in common use. Both cross-sections and uncertainties are provided in a fine multigroup structure for use in least squares adjustment applications. These cross-sections were compiled from the most recent cross-section evaluations and they have been tested with respect to their accuracy and consistency for least squares evaluations. Further, the library has been empirically tested for use in fission spectra determination as well as in the fluence and energy characterization of 14 MeV neutron sources.

For sensors included in the Comanche Peak Unit 1 surveillance program, the following uncertainties in the fission spectrum averaged cross-sections are provided in the SNLRML documentation package.

Reaction	Uncertainty
$^{63}Cu(n,\alpha)^{60}Co$	4.08-4.16%
$^{54}Fe(n,p)^{54}Mn$	3.05-3.11%
$^{58}Ni(n,p)^{58}Co$	4.49-4.56%
$^{238}U(n,f)^{137}Cs$	0.54-0.64%
$^{237}Np(n,f)^{137}Cs$	10.32-10.97%
$^{59}Co(n,\gamma)^{60}Co$	0.79-3.59%

These tabulated ranges provide an indication of the dosimetry cross-section uncertainties associated with the sensor sets used in LWR irradiations.

Calculated Neutron Spectrum

The neutron spectra input to the least squares adjustment procedure were obtained directly from the results of plant specific transport calculations for each surveillance capsule irradiation period and location. The spectrum for each capsule was input in an absolute sense (rather than as simply a relative spectral shape). Therefore, within the constraints of the assigned uncertainties, the calculated data were treated equally with the measurements.

While the uncertainties associated with the reaction rates were obtained from the measurement procedures and counting benchmarks and the dosimetry cross-section uncertainties were supplied directly with the SNLRML library, the uncertainty matrix for the calculated spectrum was constructed from the following relationship:

$$M_{gg'} = R_n^2 + R_g * R_{g'} * P_{gg'}$$

where R_n specifies an overall fractional normalization uncertainty and the fractional uncertainties R_g and $R_{g'}$ specify additional random groupwise uncertainties that are correlated with a correlation matrix given by:

$$P_{gg'} = [1-\theta]\delta_{gg'} + \theta\, e^{-H}$$

where

$$H = \frac{(g-g')^2}{2\gamma^2}$$

The first term in the correlation matrix equation specifies purely random uncertainties, while the second term describes the short-range correlations over a group range γ (θ specifies the strength of the latter term). The value of δ is 1.0 when $g = g'$, and is 0.0 otherwise.

The set of parameters defining the input covariance matrix for the Comanche Peak Unit 1 calculated spectra was as follows:

      Flux Normalization Uncertainty (R_n)   15%

      Flux Group Uncertainties (R_g, $R_{g'}$)

(E > 0.0055 MeV)	15%
(0.68 eV < E < 0.0055 MeV)	29%
(E < 0.68 eV)	52%

      Short Range Correlation (θ)

(E > 0.0055 MeV)	0.9
(0.68 eV < E < 0.0055 MeV)	0.5
(E < 0.68 eV)	0.5

      Flux Group Correlation Range (γ)

(E > 0.0055 MeV)	6
(0.68 eV < E < 0.0055 MeV)	3
(E < 0.68 eV)	2

A.1.3 Comparisons of Measurements and Calculations

Results of the least squares evaluations of the dosimetry from the Comanche Peak Unit 1 surveillance capsules withdrawn to date are provided in Tables A-5 and A-6. In Table A-5, measured, calculated, and best-estimate values for sensor reaction rates are given for each capsule. Also provided in this tabulation are ratios of the measured reaction rates to both the calculated and least squares adjusted reaction rates. These ratios of M/C and M/BE illustrate the consistency of the fit of the calculated neutron energy spectra to the measured reaction rates both before and after adjustment. In Table A-6, comparison of the calculated and best estimate values of neutron flux (E > 1.0 MeV) and iron atom displacement rate are tabulated along with the BE/C ratios observed for each of the capsules.

The data comparisons provided in Tables A-5 and A-6 show that the adjustments to the calculated spectra are relatively small and well within the assigned uncertainties for the calculated spectra, measured sensor reaction rates, and dosimetry reaction cross-sections. Further, these results indicate that the use of the least squares evaluation results in a reduction in the uncertainties associated with the exposure of the surveillance capsules. From Section 3.4 of this report, it may be noted that the uncertainty associated with the unadjusted calculation of neutron fluence (E > 1.0 MeV) and iron atom displacements at the surveillance capsule locations is specified as 12% at the 1σ level. From Table A-6, it is noted that the corresponding uncertainties associated with the least squares adjusted exposure parameters have been reduced to 6% for neutron flux (E > 1.0 MeV) and 8% for iron atom displacement rate. Again, the uncertainties from the least squares evaluation are at the 1σ level.

Further comparisons of the measurement results (from Tables A-5 and A-6) with calculations are given in Tables A-7 and A-8. These comparisons are given on two levels. In Table A-7, calculations of individual threshold sensor reaction rates are compared directly with the corresponding measurements. These threshold reaction rate comparisons provide a good evaluation of the accuracy of the fast neutron portion of the calculated energy spectra. In Table A-8, calculations of fast neutron exposure rates in terms of φ(E > 1.0 MeV) and dpa/s are compared with the best estimate results obtained from the least squares evaluation of the capsule dosimetry results. These two levels of comparison yield consistent and similar results with all measurement-to-calculation comparisons falling well within the 20% limits specified as the acceptance criteria in Regulatory Guide 1.190.

In the case of the direct comparison of measured and calculated sensor reaction rates, the M/C comparisons for fast neutron reactions range from 0.98 to 1.21 for the 10 samples included in the data set. The overall average M/C ratio for the entire set of Comanche Peak Unit 1 data is 1.10 with an associated standard deviation of 7.1%.

In the comparisons of best estimate and calculated fast neutron exposure parameters, the corresponding BE/C comparisons for the capsule data sets range from 1.05 to 1.08 for neutron flux (E > 1.0 MeV) and from 1.06 to 1.07 for iron atom displacement rate. The overall average BE/C ratios for neutron flux (E > 1.0 MeV) and iron atom displacement rate are 1.07 with a standard deviation of 1.9% and 1.06 with a standard deviation of 0.8%, respectively.

Based on these comparisons, it is concluded that the calculated fast neutron exposures provided in Section 3.2 of this report are validated for use in the assessment of the condition of the materials comprising the beltline region of the Comanche Peak Unit 1 reactor pressure vessel.

TABLE A-1

Nuclear Parameters Used In The Evaluation Of Neutron Sensors

Monitor Material	Reaction of Interest	Target Atom Fraction	90% Response Range (MeV)	Product Half-life	Fission Yield (%)
Copper	^{63}Cu (n,α)	0.6917	4.9 – 11.9	5.271 y	
Iron	^{54}Fe (n,p)	0.0585	2.1 – 8.5	312.1 d	
Nickel	^{58}Ni (n,p)	0.6808	1.5 – 8.3	70.82 d	
Uranium-238	^{238}U (n,f)	1.0000	1.3 – 6.9	30.07 y	6.02
Neptunium-237	^{237}Np (n,f)	1.0000	0.3 – 3.8	30.07 y	6.17
Cobalt-Aluminum	^{59}Co (n,γ)	0.0015	non-threshold	5.271 y	

Note: The 90% response range is defined such that, in the neutron spectrum characteristic of the Comanche Peak Unit 1 surveillance capsules, approximately 90% of the sensor response is due to neutrons in the energy range specified with approximately 5% of the total response due to neutrons with energies below the lower limit and 5% of the total response due to neutrons with energies above the upper limit.

TABLE A-2

Monthly Thermal Generation During The First Ten Fuel Cycles
Of The Comanche Peak Unit 1 Reactor
(Reactor power of 3411 MWt from startup through the end of Cycle 9,
and 3458 MWt for Cycle 10)

Year	Month	Thermal Generation (MWt-hr)	Year	Month	Thermal Generation (MWt-hr)	Year	Month	Thermal Generation (MWt-hr)
1990	4	127135	1993	4	2326657	1996	4	2149764
1990	5	745699	1993	5	2493823	1996	5	2529852
1990	6	521146	1993	6	2240371	1996	6	2457287
1990	7	1688200	1993	7	2534100	1996	7	2530409
1990	8	1515303	1993	8	2522312	1996	8	2324480
1990	9	1480019	1993	9	2443150	1996	9	2449157
1990	10	1911852	1993	10	410302	1996	10	315929
1990	11	1072991	1993	11	0	1996	11	959823
1990	12	2371846	1993	12	794163	1996	12	2536114
1991	1	2265340	1994	1	2536147	1997	1	2530064
1991	2	2053558	1994	2	2062073	1997	2	2278471
1991	3	1376052	1994	3	2490712	1997	3	2529483
1991	4	0	1994	4	2445196	1997	4	2454782
1991	5	262292	1994	5	2459767	1997	5	2531276
1991	6	2436355	1994	6	2449780	1997	6	2450992
1991	7	2399188	1994	7	2531808	1997	7	2536073
1991	8	2522559	1994	8	2506758	1997	8	2531964
1991	9	2431359	1994	9	2450190	1997	9	2449639
1991	10	156278	1994	10	2532215	1997	10	2196887
1991	11	0	1994	11	2362352	1997	11	2452982
1991	12	1234345	1994	12	2358419	1997	12	2387719
1992	1	2252734	1995	1	2531561	1998	1	2531683
1992	2	2169969	1995	2	2292522	1998	2	2287085
1992	3	2082375	1995	3	214563	1998	3	1618720
1992	4	2250441	1995	4	697465	1998	4	95044
1992	5	2371846	1995	5	2399712	1998	5	2455855
1992	6	2001084	1995	6	1934160	1998	6	2450787
1992	7	2125108	1995	7	2529901	1998	7	2533273
1992	8	2514943	1995	8	2415471	1998	8	2536024
1992	9	2439220	1995	9	2451500	1998	9	2451500
1992	10	1591109	1995	10	2494609	1998	10	2532029
1992	11	0	1995	11	2115554	1998	11	2454119
1992	12	138514	1995	12	2412212	1998	12	2532479
1993	1	1995026	1996	1	1426955	1999	1	2531767
1993	2	2269843	1996	2	1989034	1999	2	2287026
1993	3	2434962	1996	3	2524995	1999	3	2536263

TABLE A-2 cont'd

Monthly Thermal Generation During The First Ten Fuel Cycles
Of The Comanche Peak Unit 1 Reactor
(Reactor power of 3411 MWt from startup through the end of Cycle 9,
and 3458 MWt for Cycle 10)

Year	Month	Thermal Generation (MWt-hr)	Year	Month	Thermal Generation (MWt-hr)
1999	4	2450541	2002	4	2449924
1999	5	2531243	2002	5	2531606
1999	6	2454339	2002	6	2452827
1999	7	2502755	2002	7	2535591
1999	8	2520184	2002	8	2531416
1999	9	1927102	2002	9	2204280
1999	10	52213	2002	10	0
1999	11	2402258	2002	11	491755
1999	12	2536712	2002	12	1569092
2000	1	2531882	2003	1	2569381
2000	2	2372279	2003	2	2321037
2000	3	2535722	2003	3	1993314
2000	4	2450958	2003	4	2482903
2000	5	2536074	2003	5	2237613
2000	6	2454250	2003	6	2486937
2000	7	2472397	2003	7	2569748
2000	8	2535713	2003	8	2564875
2000	9	2431919	2003	9	2486184
2000	10	2539103	2003	10	2573428
2000	11	2451983	2003	11	2471970
2000	12	2518969	2003	12	2569728
2001	1	2497694	2004	1	2565329
2001	2	2290038	2004	2	2399714
2001	3	1806552	2004	3	2155520
2001	4	516742			
2001	5	2535533			
2001	6	2453317			
2001	7	2532596			
2001	8	1547417			
2001	9	2453381			
2001	10	2538204			
2001	11	2451413			
2001	12	2533492			
2002	1	2536264			
2002	2	2286146			
2002	3	2535146			

TABLE A-3

Calculated C_j Factors at the Surveillance Capsule Center
Core Midplane Elevation

Fuel Cycle	Cycle Length [EFPS]	$\varphi(E > 1.0\ \text{MeV})$ [n/cm²-s]	
		Capsule U	Capsule Y
1	2.89E+07	1.10E+11	1.02E+11
2	2.43E+07		6.54E+10
3	2.30E+07		7.22E+10
4	3.70E+07		8.39E+10
5	4.24E+07		7.03E+10
6	4.14E+07		6.45E+10
Average		1.10E+11	7.58E+10

Fuel Cycle	Cycle Length [EFPS]	C_i	
		Capsule U	Capsule Y
1	2.89E+07	1.000	1.340
2	2.43E+07		0.862
3	2.30E+07		0.952
4	3.70E+07		1.106
5	4.24E+07		0.927
6	4.14E+07		0.851
Average		1.000	1.000

TABLE A-4
Measured Sensor Activities And Reaction Rates
Surveillance Capsule U

Reaction	Location	Measured Activity (dps/g)	Saturated Activity (dps/g)	Radially Adjusted Reaction Rate (rps/atom)
^{63}Cu (n,α) ^{60}Co	Top	4.75E+04	4.60E+05	7.02E-17
	Middle	4.43E+04	4.29E+05	6.54E-17
	Bottom	4.31E+04	4.17E+05	6.37E-17
	Average			**6.64E-17**
^{54}Fe (n,p) ^{54}Mn	Top	1.24E+06	4.08E+06	6.46E-15
	Middle	1.30E+06	4.27E+06	6.77E-15
	Bottom	1.21E+06	3.98E+06	6.30E-15
	Average			**6.51E-15**
^{58}Ni (n,p) ^{58}Co	Top	7.80E+06	6.44E+07	9.21E-15
	Middle	7.31E+06	6.03E+07	8.63E-15
	Bottom	7.30E+06	6.02E+07	8.62E-15
	Average			**8.82E-15**
^{238}U (n,f) ^{137}Cs (Cd)	Middle	1.50E+05	7.31E+06	4.80E-14
	Including ^{235}U, ^{239}Pu, and γ fission corrections:			**4.04E-14**
^{237}Np (n,f) ^{137}Cs (Cd)	Middle	1.28E+06	6.24E+07	3.98E-13
	Including γ fission correction:			**3.94E-13**
^{59}Co (n,γ) ^{60}Co	Top	9.47E+06	9.17E+07	5.98E-12
	Top	8.18E+06	7.92E+07	5.17E-12
	Middle	9.40E+06	9.10E+07	5.94E-12
	Middle	7.97E+06	7.72E+07	5.03E-12
	Bottom	9.20E+06	8.91E+07	5.81E-12
	Average			**5.59E-12**
^{59}Co (n,γ) ^{60}Co (Cd)	Top	4.85E+06	4.70E+07	3.06E-12
	Middle	4.93E+06	4.77E+07	3.11E-12
	Average			**3.09E-12**

Notes: 1) Measured specific activities are indexed to a counting date of April 13, 1992.

2) The average ^{238}U (n,f) reaction rate of 4.04E-14 includes a correction factor of 0.872 to account for plutonium build-in and an additional factor of 0.966 to account for photo-fission effects in the sensor.

3) The average ^{237}Np (n,f) reaction rate of 3.94E-13 includes a correction factor of 0.990 to account for photo-fission effects in the sensor.

4) Reaction rates referenced to the Cycle 1 Rated Reactor Power of 3411 MWt.

TABLE A-4 cont'd
Measured Sensor Activities And Reaction Rates
Surveillance Capsule Y

Reaction	Location	Measured Activity (dps/g)	Saturated Activity (dps/g)	Radially Adjusted Reaction Rate (rps/atom)
^{63}Cu (n,α) ^{60}Co	Top	1.64E+05	3.38E+05	5.16E-17
	Middle	1.46E+05	3.01E+05	4.59E-17
	Bottom	1.45E+05	2.91E+05	4.56E-17
	Average			**4.77E-17**
^{54}Fe (n,p) ^{54}Mn	Top	1.77E+06	3.19E+06	5.06E-15
	Middle	1.61E+06	2.91E+06	4.61E-15
	Bottom	1.63E+06	2.94E+06	4.66E-15
	Average			**4.78E-15**
^{58}Ni (n,p) ^{58}Co	Top	7.49E+06	4.84E+07	6.93E-15
	Middle	6.76E+06	4.37E+07	6.26E-15
	Bottom	6.84E+06	4.42E+07	6.33E-15
	Average			**6.51E-15**
^{238}U (n,f) ^{137}Cs (Cd)	Middle	7.28E+05	5.58E+06	3.67E-14
	Including ^{235}U, ^{239}Pu, and γ fission corrections:			**2.93E-14**
^{237}Np (n,f) ^{137}Cs (Cd)	Middle	5.31E+06	4.07E+07	2.60E-13
	Including γ fission correction:			**2.57E-13**
^{59}Co (n,γ) ^{60}Co	Top	2.32E+07	4.79E+07	3.12E-12
	Top	2.74E+07	5.65E+07	3.69E-12
	Middle	2.12E+07	4.37E+07	2.85E-12
	Middle	2.60E+07	5.36E+07	3.50E-12
	Bottom	2.50E+07	5.16E+07	3.36E-12
	Bottom	2.65E+07	5.47E+07	3.57E-12
	Average			**3.35E-12**
^{59}Co (n,γ) ^{60}Co (Cd)	Top	1.46E+07	3.01E+07	1.97E-12
	Middle	1.41E+07	2.91E+07	1.90E-12
	Bottom	1.48E+07	3.05E+07	1.99E-12
	Average			**1.95E-12**

Notes: 1) Measured specific activities are indexed to a counting date of September 8, 1998.
2) The average ^{238}U (n,f) reaction rate of 2.93E-14 includes a correction factor of 0.826 to account for plutonium build-in and an additional factor of 0.967 to account for photo-fission effects in the sensor.
3) The average ^{237}Np (n,f) reaction rate of 2.57E-13 includes a correction factor of 0.990 to account for photo-fission effects in the sensor.
4) Reaction rates referenced to the Cycles 1-6 Rated Reactor Power of 3411 MWt.

TABLE A-5

Comparison of Measured, Calculated, and Best Estimate
Reaction Rates At The Surveillance Capsule Center

Capsule U

Reaction	Reaction Rate [rps/atom]			M/C	M/BE
	Measured	Calculated	Best Estimate		
$^{63}Cu(n,\alpha)^{60}Co$	6.64E-17	5.63E-17	6.33E-17	1.18	1.05
$^{54}Fe(n,p)^{54}Mn$	6.51E-15	6.42E-15	6.70E-15	1.01	0.97
$^{58}Ni(n,p)^{58}Co$	8.82E-15	9.03E-15	9.29E-15	0.98	0.95
$^{238}U(n,f)^{137}Cs$ (Cd)	4.04E-14	3.50E-14	3.65E-14	1.15	1.11
$^{237}Np(n,f)^{137}Cs$ (Cd)	3.94E-13	3.46E-13	3.78E-13	1.14	1.04
$^{59}Co(n,\gamma)^{60}Co$	5.59E-12	4.99E-12	5.51E-12	1.12	1.01
$^{59}Co(n,\gamma)^{60}Co$ (Cd)	3.09E-12	3.47E-12	3.14E-12	0.89	0.98

Note: See Section A.1.2 for details describing the Best Estimate (BE) reaction rates.

Capsule Y

Reaction	Reaction Rate [rps/atom]			M/C	M/BE
	Measured	Calculated	Best Estimate		
$^{63}Cu(n,\alpha)^{60}Co$	4.77E-17	4.16E-17	4.63E-17	1.15	1.03
$^{54}Fe(n,p)^{54}Mn$	4.78E-15	4.55E-15	4.87E-15	1.05	0.98
$^{58}Ni(n,p)^{58}Co$	6.51E-15	6.37E-15	6.75E-15	1.02	0.96
$^{238}U(n,f)^{137}Cs$ (Cd)	2.93E-14	2.43E-14	2.61E-14	1.21	1.12
$^{237}Np(n,f)^{137}Cs$ (Cd)	2.57E-13	2.36E-13	2.55E-13	1.09	1.01
$^{59}Co(n,\gamma)^{60}Co$	3.35E-12	3.29E-12	3.31E-12	1.02	1.01
$^{59}Co(n,\gamma)^{60}Co$ (Cd)	1.95E-12	2.30E-12	1.98E-12	0.85	0.98

Note: See Section A.1.2 for details describing the Best Estimate (BE) reaction rates.

TABLE A-6

Comparison of Calculated and Best Estimate Exposure Rates
At The Surveillance Capsule Center

Capsule ID	$\varphi(E > 1.0 \text{ MeV}) \text{ [n/cm}^2\text{-s]}$			
	Calculated	Best Estimate	Uncertainty (1σ)	BE/C
U	1.10E+11	1.16E+11	6%	1.05
Y	7.58E+10	8.21E+10	6%	1.08

Note: Calculated results are based on the synthesized transport calculations taken at the core midplane following the completion of each respective capsules irradiation period and are the average neutron exposure over the irradiation period for each capsule. See Section A.1.2 for details describing the Best Estimate exposure rates.

Capsule ID	Iron Atom Displacement Rate [dpa/s]			
	Calculated	Best Estimate	Uncertainty (1σ)	BE/C
U	2.16E-10	2.28E-10	8%	1.06
Y	1.48E-10	1.58E-10	8%	1.07

Note: Calculated results are based on the synthesized transport calculations taken at the core midplane following the completion of each respective capsules irradiation period and are the average neutron exposure over the irradiation period for each capsule. See Section A.1.2 for details describing the Best Estimate exposure rates.

TABLE A-7

Comparison of Measured/Calculated (M/C) Sensor Reaction Rate
Ratios Including all Fast Neutron Threshold Reactions

Reaction	M/C Ratio	
	Capsule U	Capsule Y
$^{63}Cu(n,\alpha)^{60}Co$	1.18	1.15
$^{54}Fe(n,p)^{54}Mn$	1.01	1.05
$^{58}Ni(n,p)^{58}Co$	0.98	1.02
$^{238}U(n,p)^{137}Cs$ (Cd)	1.15	1.21
$^{237}Np(n,f)^{137}Cs$ (Cd)	1.14	1.09
Average	1.09	1.10
% Standard Deviation	8.3	6.7

Note: The overall average M/C ratio for the set of 10 sensor measurements is 1.10
with an associated standard deviation of 7.1%.

TABLE A-8

Comparison of Best Estimate/Calculated (BE/C) Exposure Rate Ratios

Capsule ID	BE/C Ratio	
	$\varphi(E > 1.0 \text{ MeV})$	dpa/s
U	1.05	1.06
Y	1.08	1.07
Average	1.07	1.06
% Standard Deviation	1.9	0.8

Appendix A References

A-1.   Regulatory Guide RG-1.190, "Calculational and Dosimetry Methods for Determining Pressure Vessel Neutron Fluence," U. S. Nuclear Regulatory Commission, Office of Nuclear Regulatory Research, March 2001.

A-2.   WCAP-13422, "Analysis of Capsule U from the Texas Utilities Electric Company Comanche Peak Unit No. 1 Reactor Vessel Radiation Surveillance Program," July 1992.

A-3.   WCAP-15144, "Analysis of Capsule Y from the TU Electric Company Comanche Peak Unit 1 Reactor Vessel Radiation Surveillance Program," January 1999.

A-4.   A. Schmittroth, *FERRET Data Analysis Core*, HEDL-TME 79-40, Hanford Engineering Development Laboratory, Richland, WA, September 1979.

A-5.   RSIC Data Library Collection DLC-178, "SNLRML Recommended Dosimetry Cross-Section Compendium," July 1994.

APPENDIX B

Thermal Stress Intensity Factors (K_{It})

The following page contain the thermal stress intensity factors (K_{It}) for the maximum heatup and cooldown rates at 36 EFPY. The vessel radius to the $\frac{1}{4}$T and $\frac{3}{4}$T locations are as follows:

- 1/4T Radius = 88.818"

- 3/4T Radius = 93.133"

TABLE B1

K_{It} Values for 100°F/hr Heatup Curve (36 EFPY)

Water Temp. (°F)	Vessel Temperature @ 1/4T Location for 100°F/hr Heatup (°F)	1/4T Thermal Stress Intensity Factor (KSI SQ. RT. IN.)	Vessel Temperature @ 3/4T Location for 100°F/hr Heatup (°F)	3/4T Thermal Stress Intensity Factor (KSI SQ. RT. IN.)
60	56	-0.9955	55	0.4729
65	59	-2.4527	55	1.4376
70	62	-3.7136	56	2.4259
75	65	-4.9121	57	3.3570
80	68	-5.9484	59	4.1917
85	72	-6.8957	61	4.9397
90	76	-7.7187	63	5.6022
95	80	-8.4708	65	6.1958
100	84	-9.1295	68	6.7232
105	88	-9.7286	71	7.1945
110	92	-10.2561	75	7.6153
115	97	-10.7377	78	7.9942
120	101	-11.1644	82	8.3345
125	106	-11.5552	85	8.6415
130	110	-11.9029	89	8.9183
135	115	-12.2227	93	9.1691
140	119	-12.5087	97	9.3963
145	124	-12.7732	102	9.6032
150	129	-13.0109	106	9.7917
155	133	-13.2322	110	9.9643
160	138	-13.4323	115	10.1225
165	143	-13.6197	119	10.2683
170	147	-13.7903	123	10.4028
175	152	-13.9514	128	10.5277
180	157	-14.0989	132	10.6437
185	162	-14.2392	137	10.7522
190	167	-14.3688	142	10.8537
195	172	-14.4928	146	10.9492
200	176	-14.6082	151	11.0394
205	181	-14.7196	156	11.1249
210	186	-14.8239	160	11.2061

Note: At the lowest temperatures (T = to 60°F to 90°F), the heatup curve is limited by the 3/4T pressure at T = 90°F. In that temperature range, considering the raw pressures at 1/4T, 3/4T and SS, the curve would be limited by Steady State at T = 60°F and 65°F, then by the 3/4T location there after.

TABLE B2

K_{lt} Values for 100°F/hr Cooldown Curve (36 EFPY)

Water Temp. (°F)	Vessel Temperature @ 1/4T Location for 100°F/hr Cooldown (°F)	100°F/hr Cooldown 1/4T Thermal Stress Intensity Factor (KSI SQ. RT. IN.)
170	196	16.6130
165	191	16.5432
160	186	16.4738
155	181	16.4039
150	176	16.3346
145	171	16.2648
140	166	16.1955
135	161	16.1258
130	156	16.0566
125	151	15.9870
120	146	15.9179
115	140	15.8486
110	135	15.7797
105	130	15.7105
100	125	15.6419
95	120	15.5730
90	115	15.5045
85	110	15.4359
80	105	15.3677
75	100	15.2993
70	95	15.2314
65	90	15.1633
60	84	15.0949

Note: At temperatures larger than T = 90°F, the 100°F/hr cooldown curve is limited by a smaller cooldown rate or Steady State.